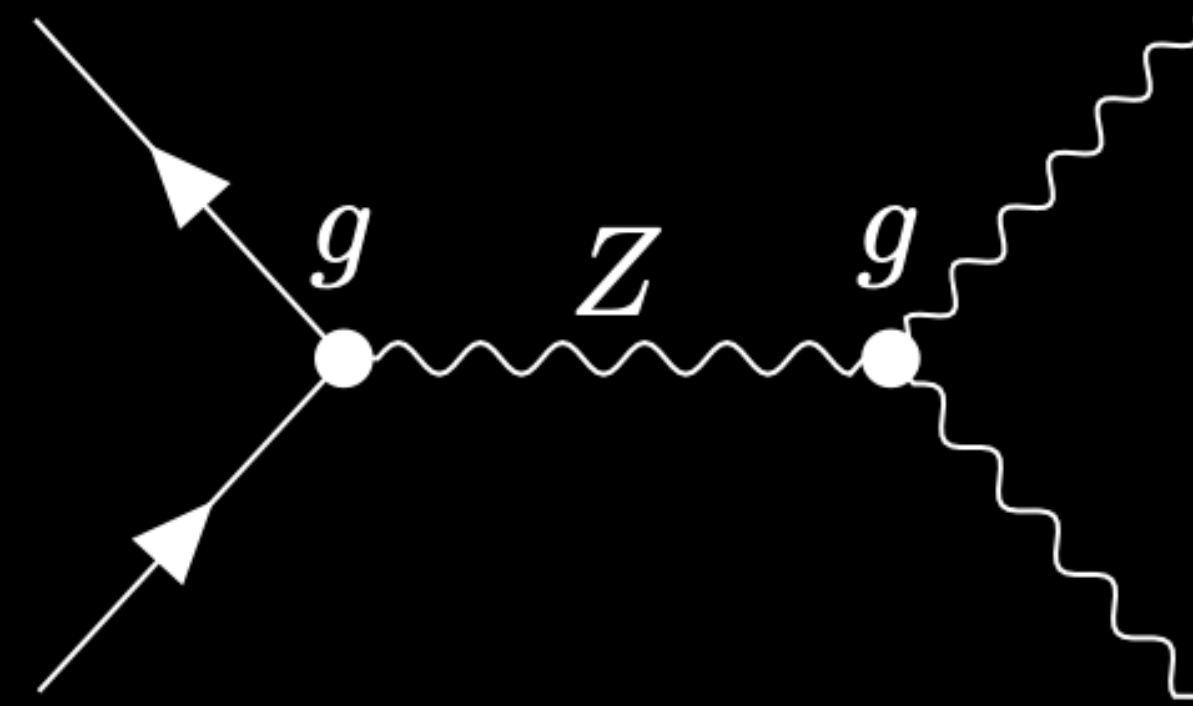
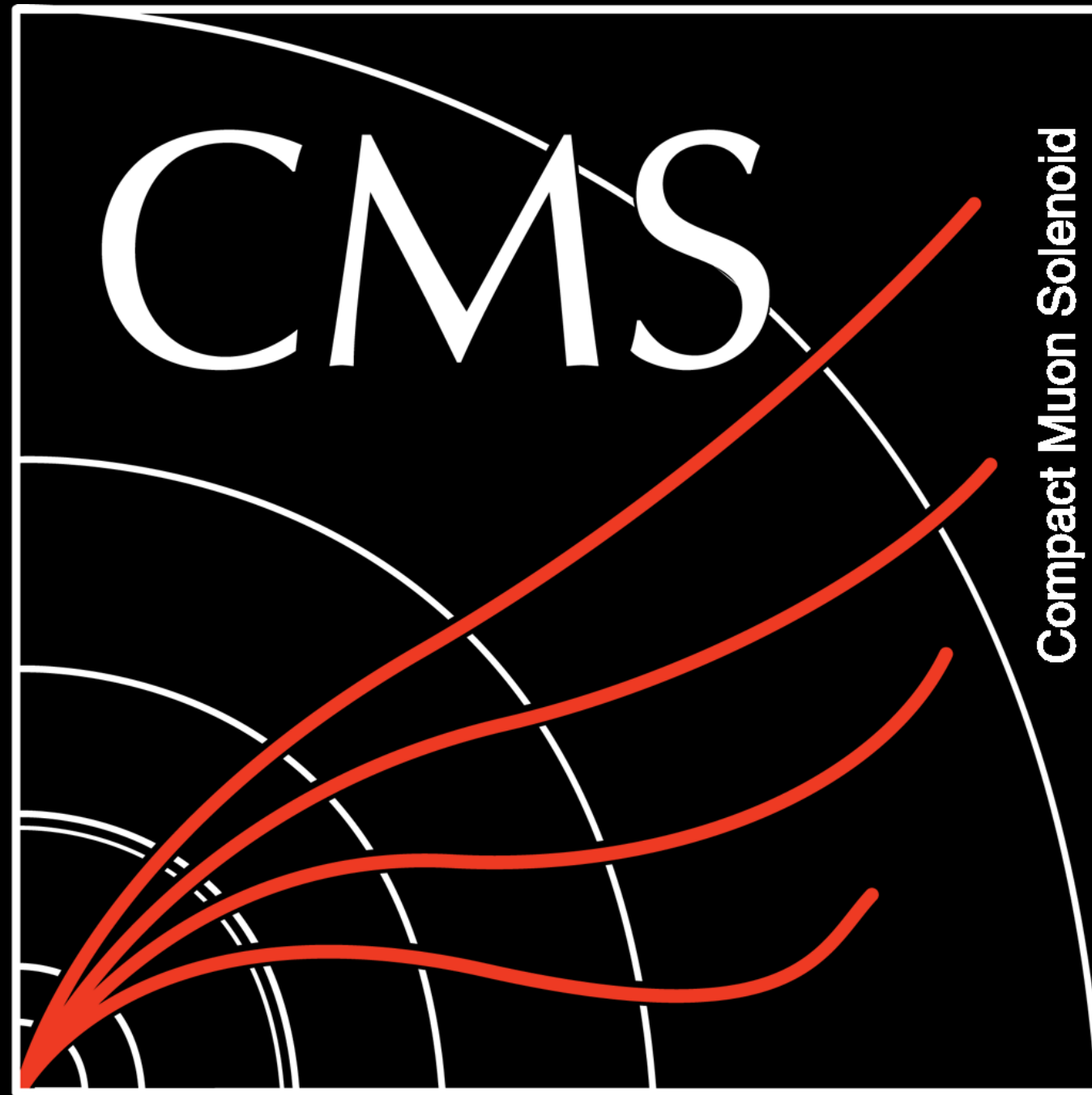


Recent diboson and polarization measurements at CMS



Saptaparna Bhattacharya

Northwestern University, Humboldt Fellow

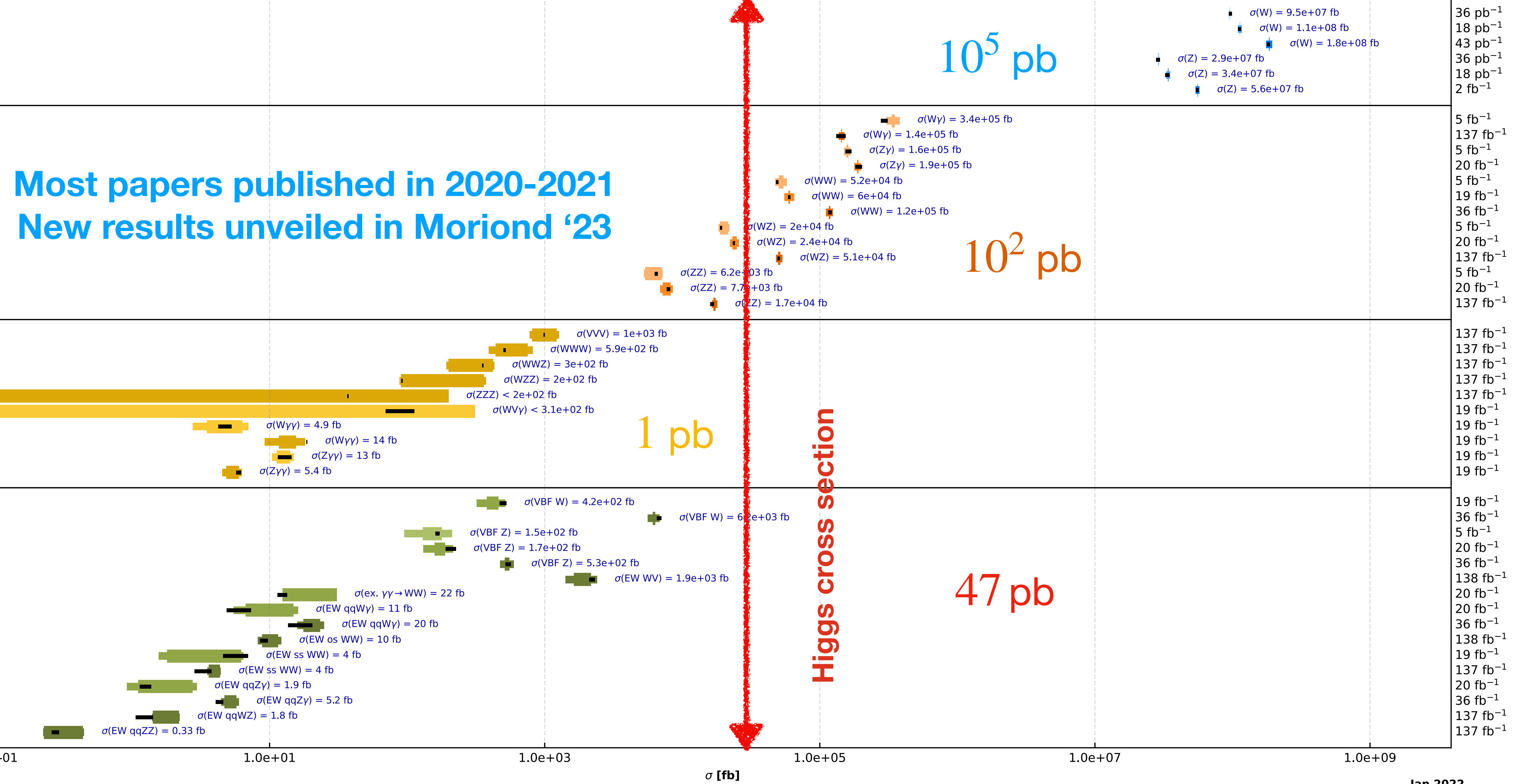
LHCP 2023, Belgrade Serbia



Overview of CMS cross section results

CMS preliminary

18 pb⁻¹ - 138 fb⁻¹ (7,8,13 TeV)



Category	Process	Energy	Reference
Electroweak	W	7 TeV	JHEP 10 (2011) 132
	W	8 TeV	PRL 112 (2014) 191802
	W	13 TeV	SMP-15-004
	Z	7 TeV	JHEP 10 (2011) 132
	Z	8 TeV	PRL 112 (2014) 191802
	Z	13 TeV	SMP-15-011
di-Boson	Wγ	7 TeV	PRD 89 (2014) 092005
	Wγ	13 TeV	PRL 126 252002 (2021)
	Zγ	7 TeV	PRD 89 (2014) 092005
	Zγ	8 TeV	JHEP 04 (2015) 164
	WW	7 TeV	EPJC 73 (2013) 2610
	WW	8 TeV	EPJC 76 (2016) 401
	WW	13 TeV	PRD 102 092001 (2020)
	WZ	7 TeV	EPJC 77 (2017) 236
	WZ	8 TeV	EPJC 77 (2017) 236
	WZ	13 TeV	Submitted to JHEP
	ZZ	7 TeV	JHEP 01 (2013) 063
	ZZ	8 TeV	PLB 740 (2015) 250
	ZZ	13 TeV	EPJC 81 (2021) 200
	tri-Boson	VVV	13 TeV
WWW		13 TeV	PRL 125 151802 (2020)
WWZ		13 TeV	PRL 125 151802 (2020)
WZZ		13 TeV	PRL 125 151802 (2020)
ZZZ		13 TeV	PRL 125 151802 (2020)
WVγ		8 TeV	PRD 90 032008 (2014)
Wγγ		8 TeV	JHEP 10 (2017) 072
Wγγ		13 TeV	JHEP 10 (2021) 174
Zγγ		8 TeV	JHEP 10 (2017) 072
Zγγ		13 TeV	JHEP 10 (2021) 174
VBF and VBS	VBF W	8 TeV	JHEP 11 (2016) 147
	VBF W	13 TeV	EPJC 80 (2020) 43
	VBF Z	7 TeV	JHEP 10 (2013) 101
	VBF Z	8 TeV	EPJC 75 (2015) 66
	VBF Z	13 TeV	EPJC 78 (2018) 589
	EW WW	13 TeV	Submitted to PLB
	ex. γγ → WW	8 TeV	JHEP 08 (2016) 119
	EW qqWγ	8 TeV	JHEP 06 (2017) 106
	EW qqWγ	13 TeV	PLB 811 (2020) 135988
	EW os WW	13 TeV	SMP-21-001
	EW ss WW	8 TeV	PRL 114 051801 (2015)
	EW ss WW	13 TeV	PRL 120 081801 (2018)
	EW qqZγ	8 TeV	PLB 770 (2017) 380
	EW qqZγ	13 TeV	PRD 104 072001 (2021)
	EW qqWZ	13 TeV	PLB 809 (2020) 135710
	EW qqZZ	13 TeV	PLB 812 (2020) 135992

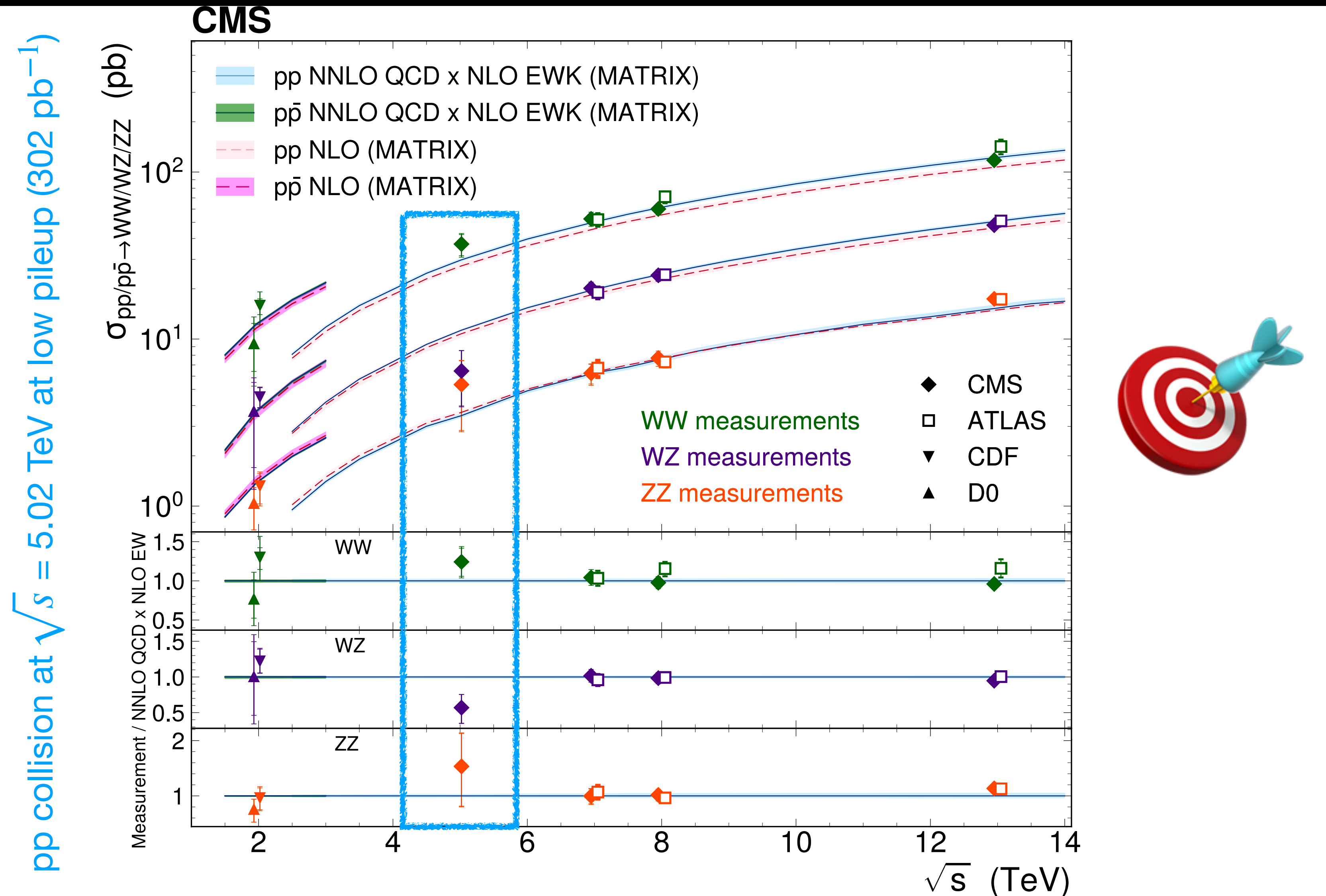
Measured cross sections and exclusion limits at 95% C.L.
See here for all cross section summary plots

Inner colored bars statistical uncertainty, outer narrow bars statistical+systematic uncertainty
Light colored bars: 7 TeV, Medium bars: 8 TeV, Dark bars: 13 TeV, Black bars: theory prediction

Jan 2022

Span several orders of magnitude!

Diboson cross section measurements at several center of mass energies (\sqrt{s})



Recent diboson and polarization measurements at CMS

Polarization Diboson Recent

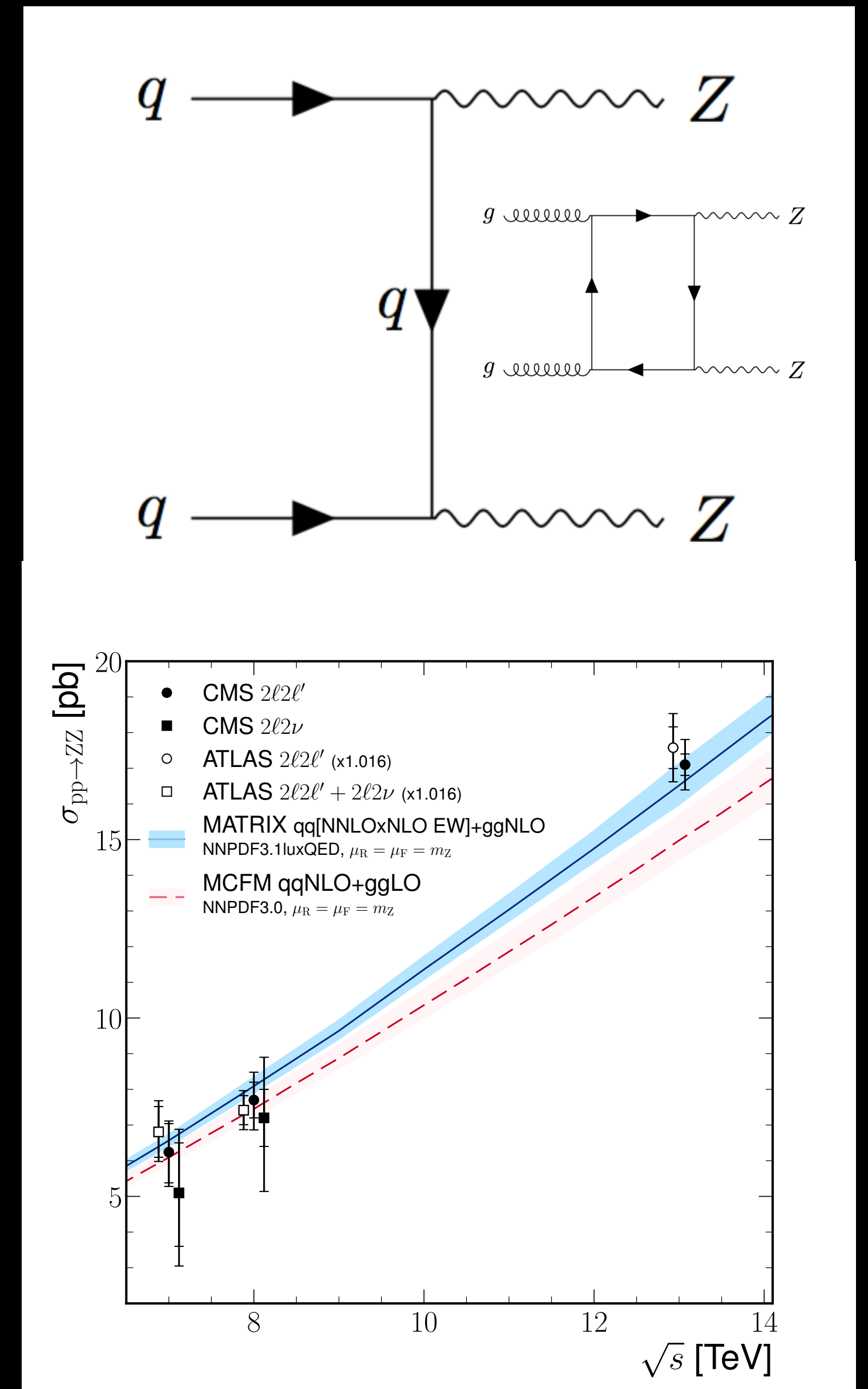
- SMP-22-001: Measurement of the $ZZ(4l) + \text{jets}$
- SMP-21-014: $\gamma\gamma \rightarrow W^+W^-$ and $\gamma\gamma \rightarrow ZZ$
- SMP-20-014: Measurement of the WZ process
- SMP-18-010: τ polarization in Z-boson decays



When an AI thinks about
“Dibosons at the precision realm”

Hot off the press! Measurement of the ZZ process

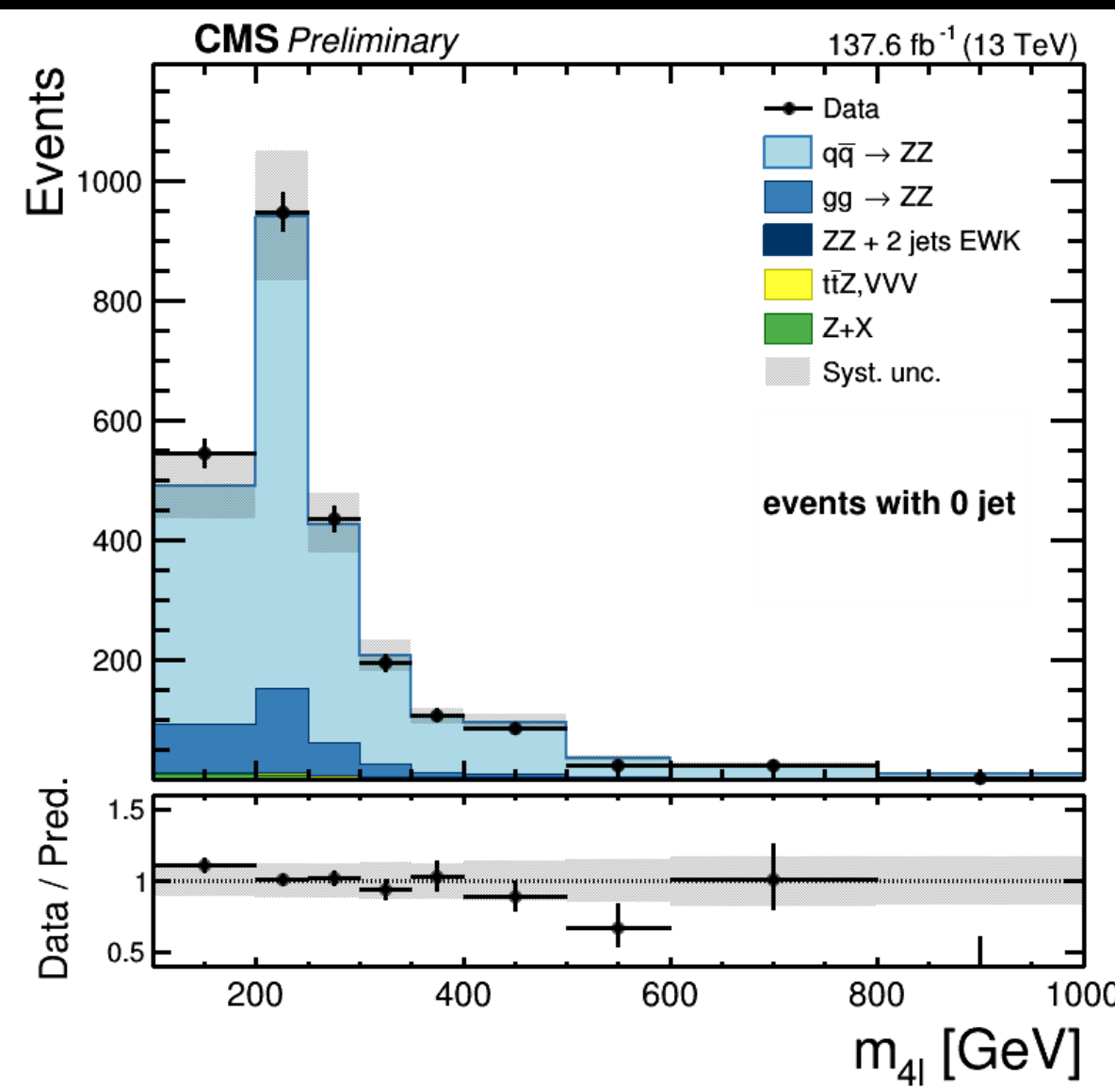
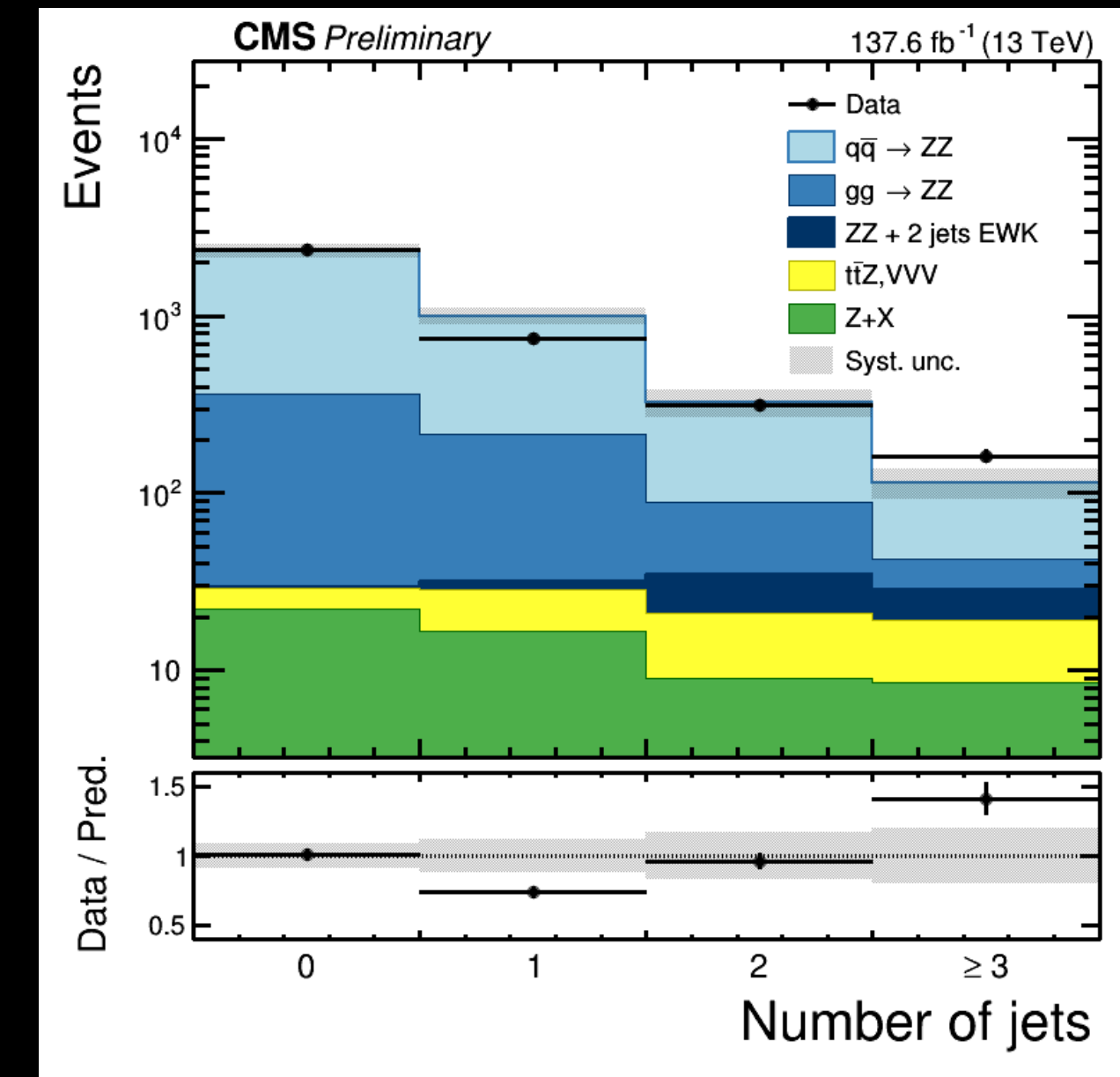
- Measurement of ZZ production in 4 lepton final state
 - No s-channel production — forbidden in the SM
 - Loop effects — up to 10% contribution
- Inclusive cross section studied in detail previously
- **First differential cross sections measured** as a function of:
 - number of jets and properties of the jets (p_T and $|\eta|$)
 - invariant mass of the highest p_T and the second highest p_T jets
 - $\Delta\eta$ of the highest p_T and the second highest p_T jets
 - m_{4l} as a function of different jet multiplicities
- New results compared with the state-of-the-art next-to-next-to-leading order (NNLO) and parton shower (PS) predictions using MiNNLO_{PS}



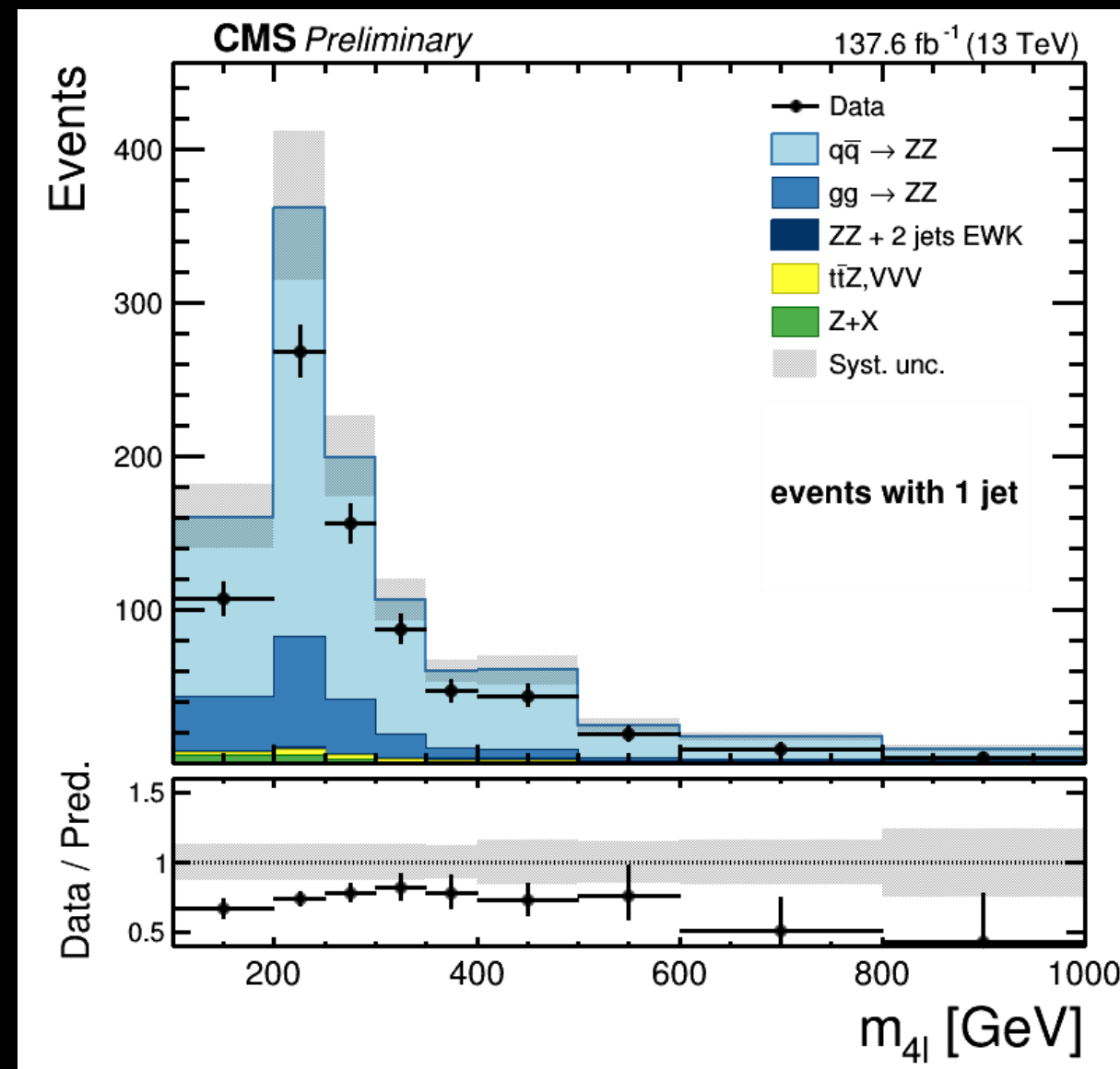
Hot off the press!

Measurement of the ZZ process

- Predictions over-estimate data → largest discrepancy for highest p_T jet with $p_T < 100$ GeV
- Shape of distributions described well by predictions → normalization is not
- Large uncertainty from QCD scales — envelope of μ_F and μ_R scale variations
 $1/4 < \mu_R/\mu_F < 4$



Data agrees with prediction



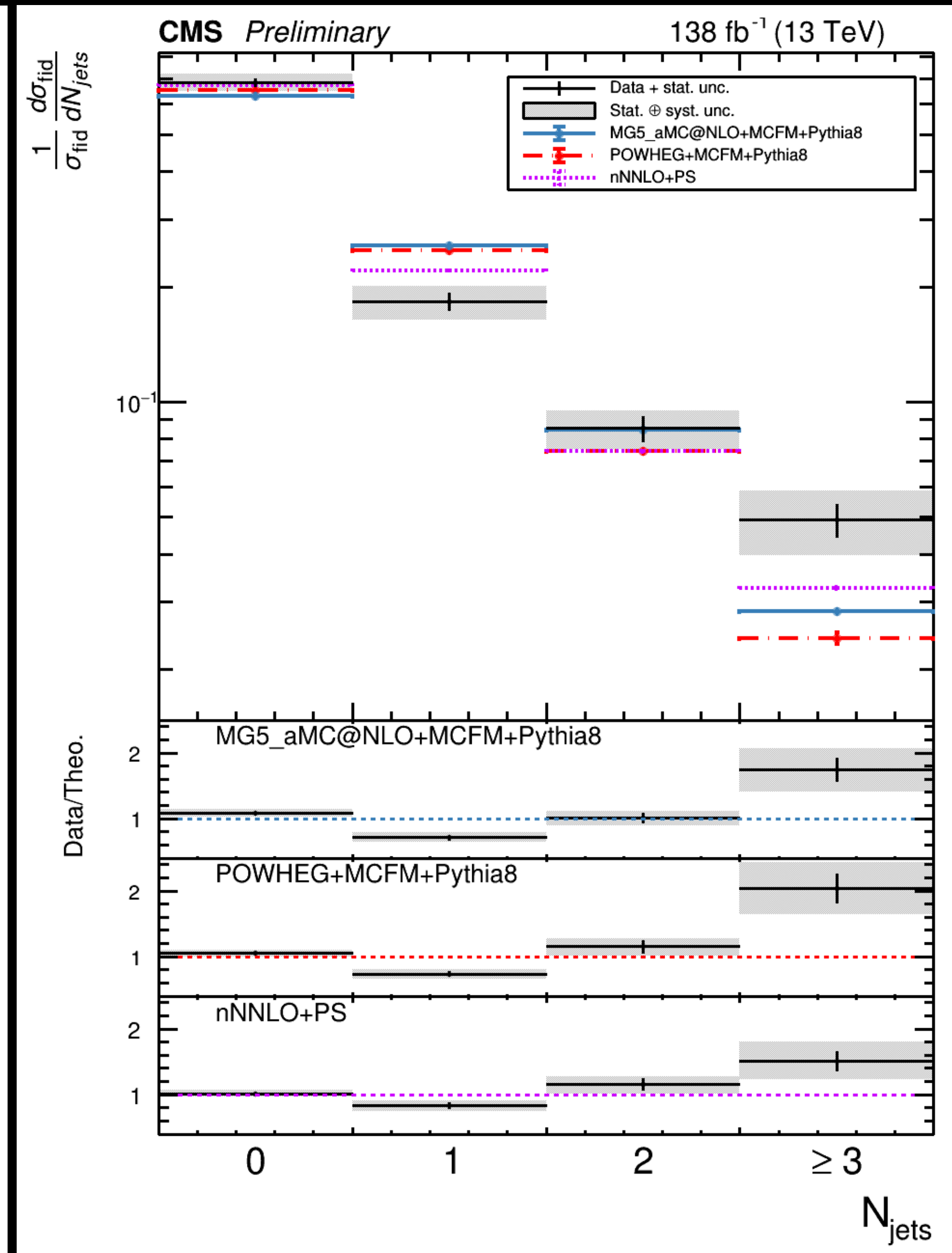
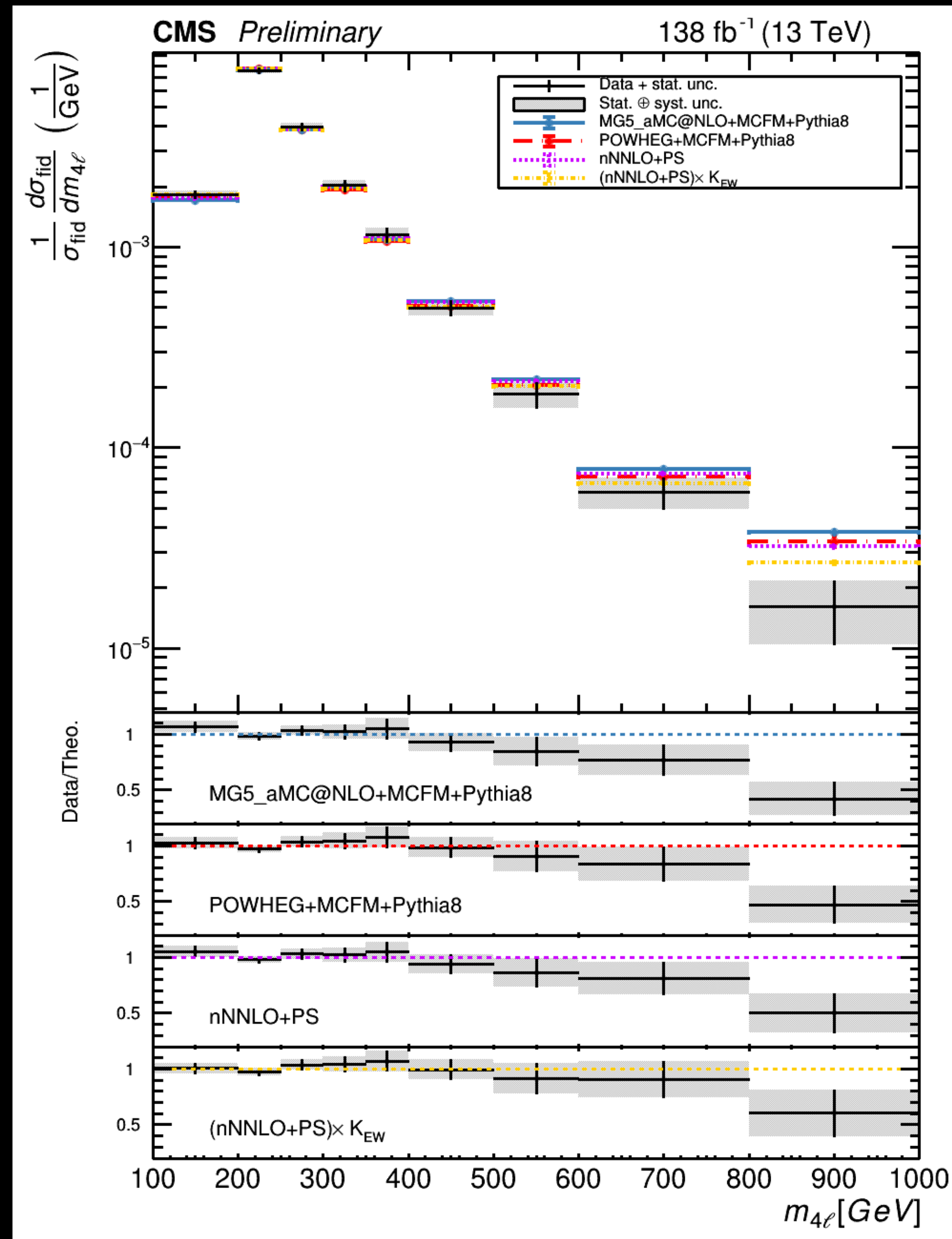
Data disagrees with prediction

Systematic source	$m_{4\ell}$ with all jets	0 jet	1 jet	2 jets	3 and more jets
Trigger	-	-	-	-	-
Electron Efficiency	0.42 %	0.38 %	0.66 %	0.36 %	0.26 %
Muon Efficiency	0.05 %	0.06 %	0.07 %	0.09 %	0.08 %
Jet energy resolution	0.0	0.07 %	1.72 %	1.65 %	0.8 %
JES correction	0.0	0.17 %	1.77 %	1.95 %	0.97 %
Reducible background	0.18 %	0.18 %	0.32 %	0.33 %	0.96 %
Pileup	0.02 %	0.05 %	0.11 %	0.13 %	0.35 %
Luminosity	0.01 %	0.01 %	0.02 %	0.02 %	0.05 %
Monte Carlo choice	0.35 %	0.65 %	0.94 %	0.48 %	0.35 %
gg cross section	0.02 %	0.03 %	0.09 %	0.06 %	0.09 %
QCD Scales	0.15 %	0.16 %	0.58 %	0.54 %	0.62 %
PDF	0.05 %	0.05 %	0.15 %	0.15 %	0.21 %
α_S	0.02 %	0.01 %	0.05 %	0.03 %	0.02 %

Hot off the press!

Measurement of the ZZ process – Unfolded distributions

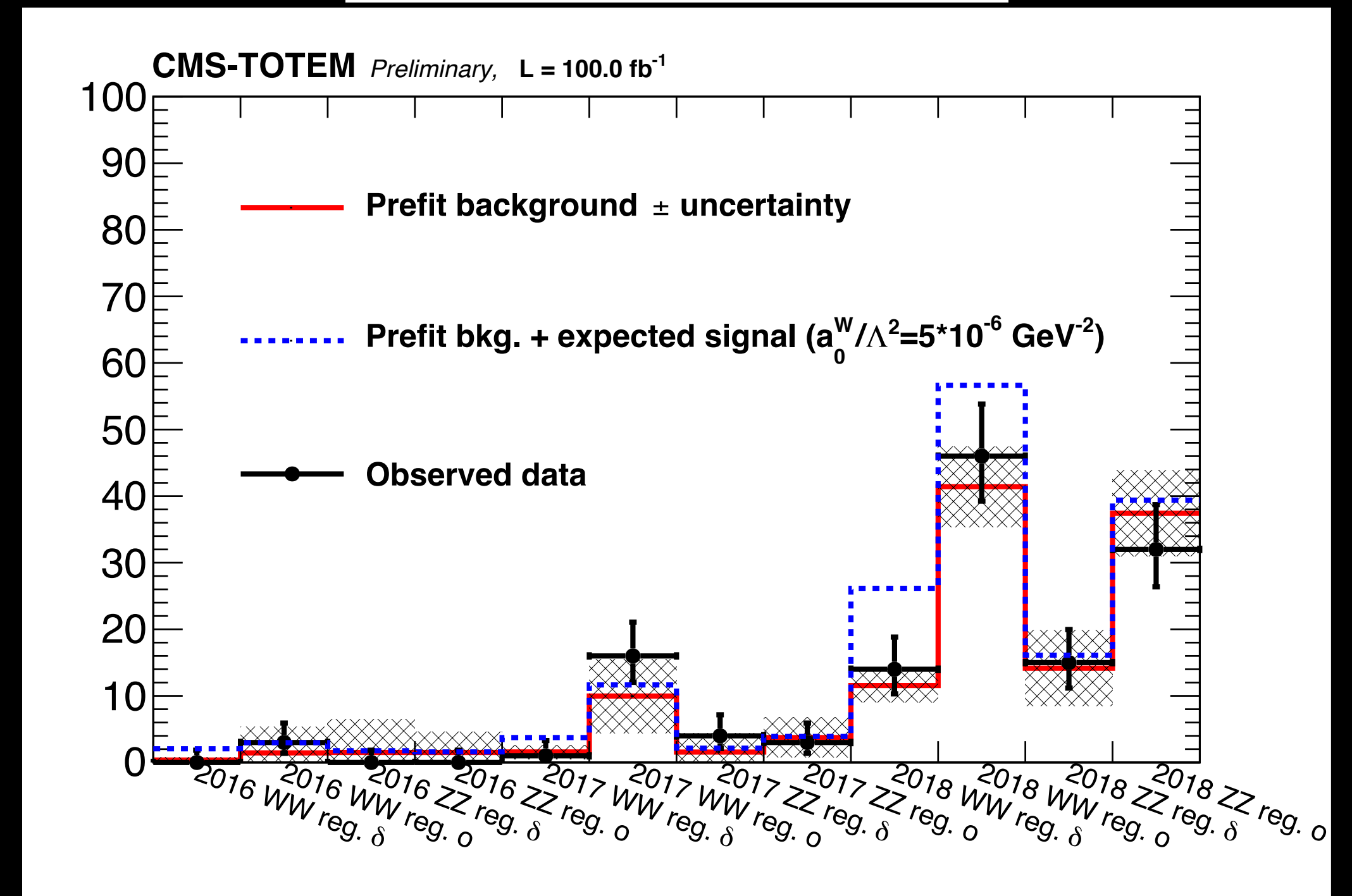
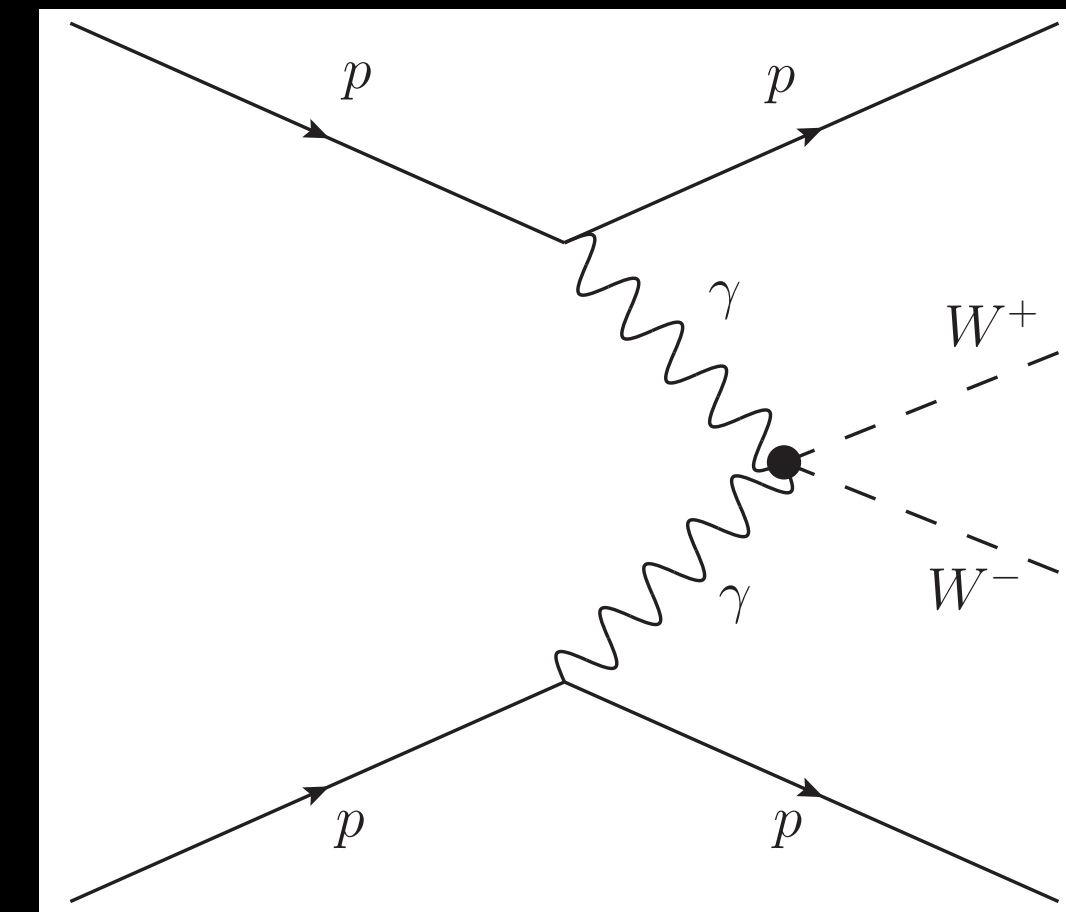
- Differential cross sections normalized to the fiducial cross sections
- On-shell Z-boson requirement applied ($60 < m_{Z_1, Z_2} < 120$)
- Comparisons with:
 - **Madgraph5_aMC@NLO** ($q\bar{q} \rightarrow ZZ$)+**MCFM** ($gg \rightarrow ZZ$)+**POWHEG** ($H \rightarrow ZZ$)
 - **POWHEG** ($q\bar{q} \rightarrow ZZ$) +**MCFM** ($gg \rightarrow ZZ$) +**POWHEG** ($H \rightarrow ZZ$)
 - Both predictions include Madgraph electro-weak corrections
 - **NNLO+PS**
 - **NNLO+PS with electroweak corrections**





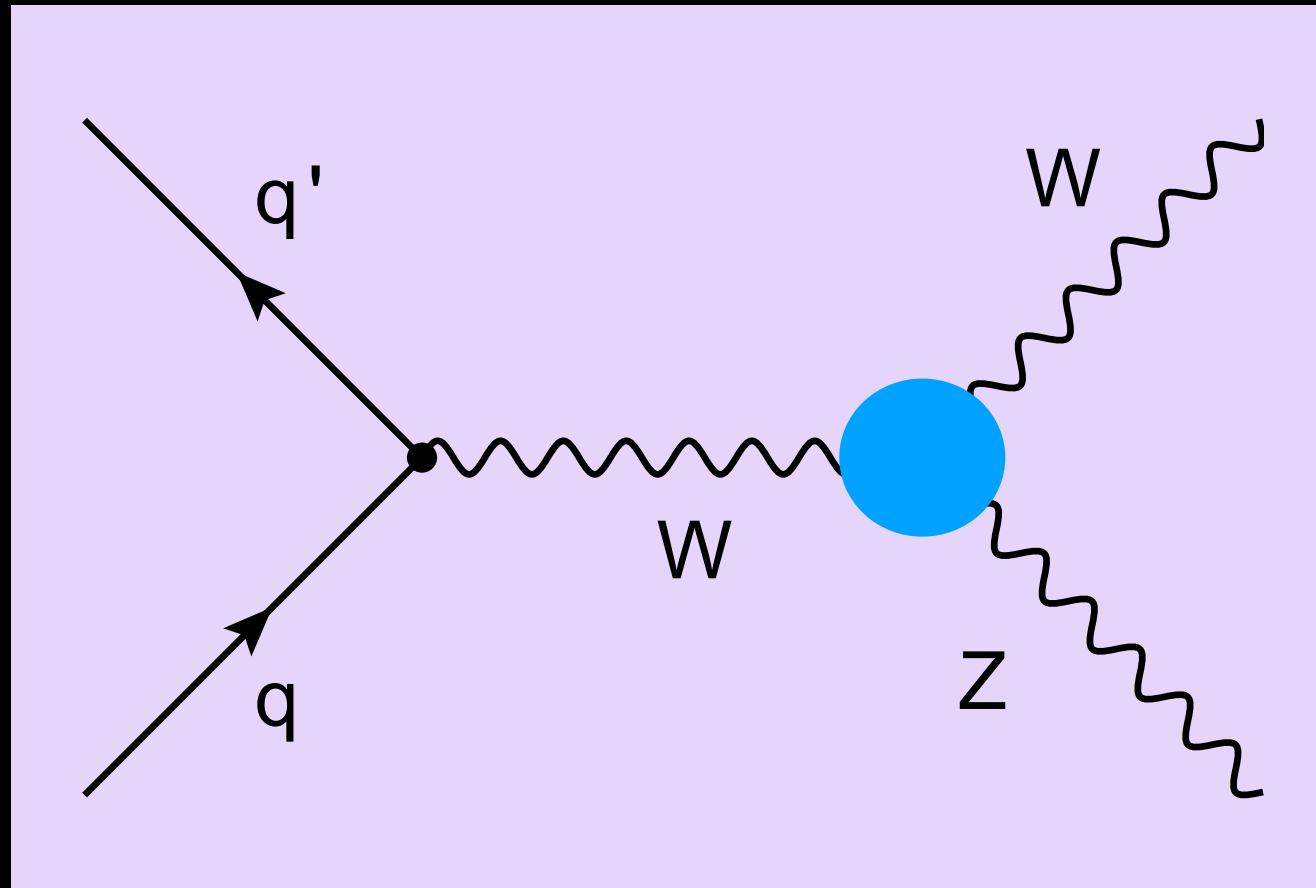
Search for exclusive $\gamma\gamma \rightarrow WW$ and $\gamma\gamma \rightarrow ZZ$ production in final states with jets and forward protons

- Both protons tagged by the precision proton spectrometer (PPS)
- The $\gamma\gamma \rightarrow WW$ process allows the study of the quartic coupling
- Events selected based on properties of jets, the protons and their correlation
- First search for anomalous high-mass $\gamma\gamma \rightarrow WW$ and $\gamma\gamma \rightarrow ZZ$ using reconstructed forward protons
- Limits 15-20x more stringent than previous results

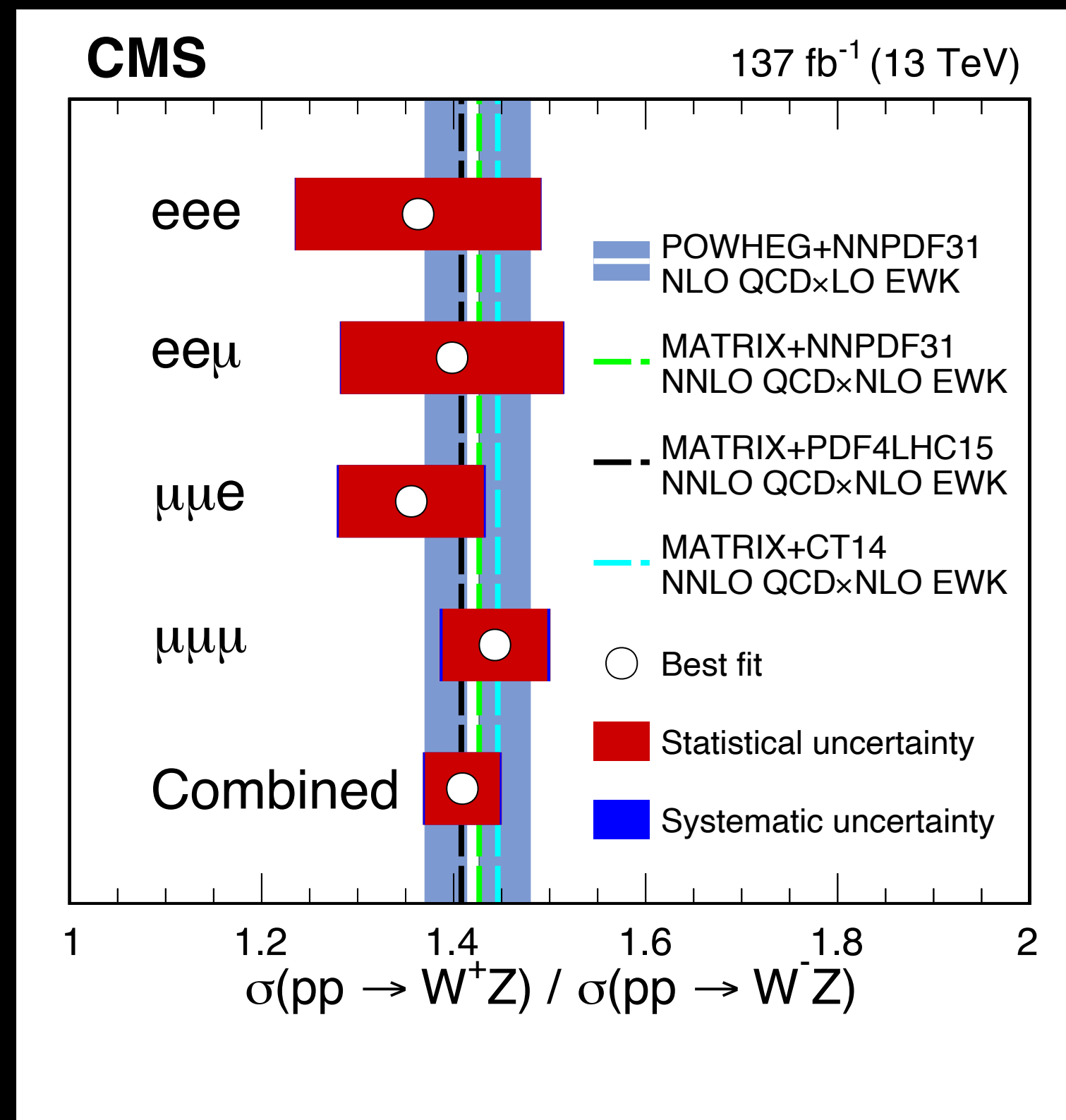


[arXiv:2211.16320](https://arxiv.org/abs/2211.16320)

Measurement of the WZ process



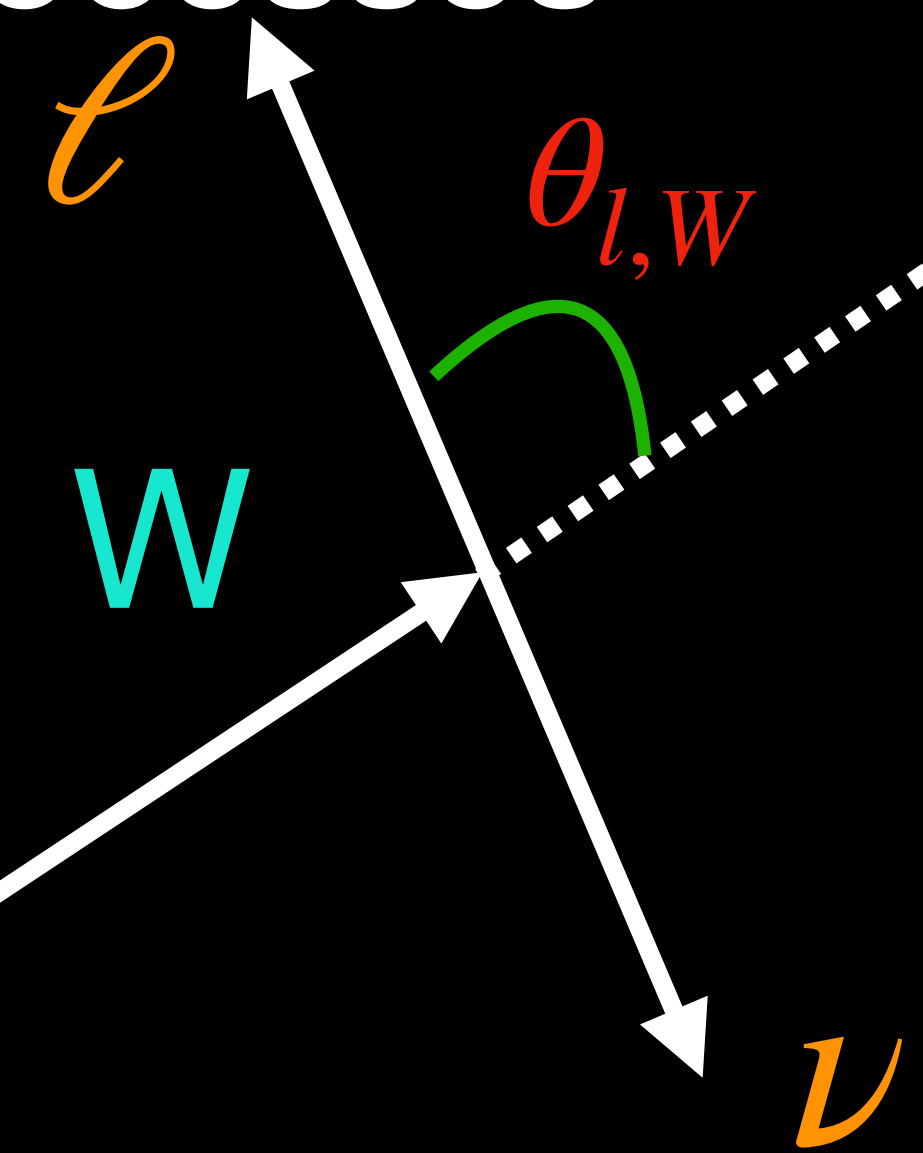
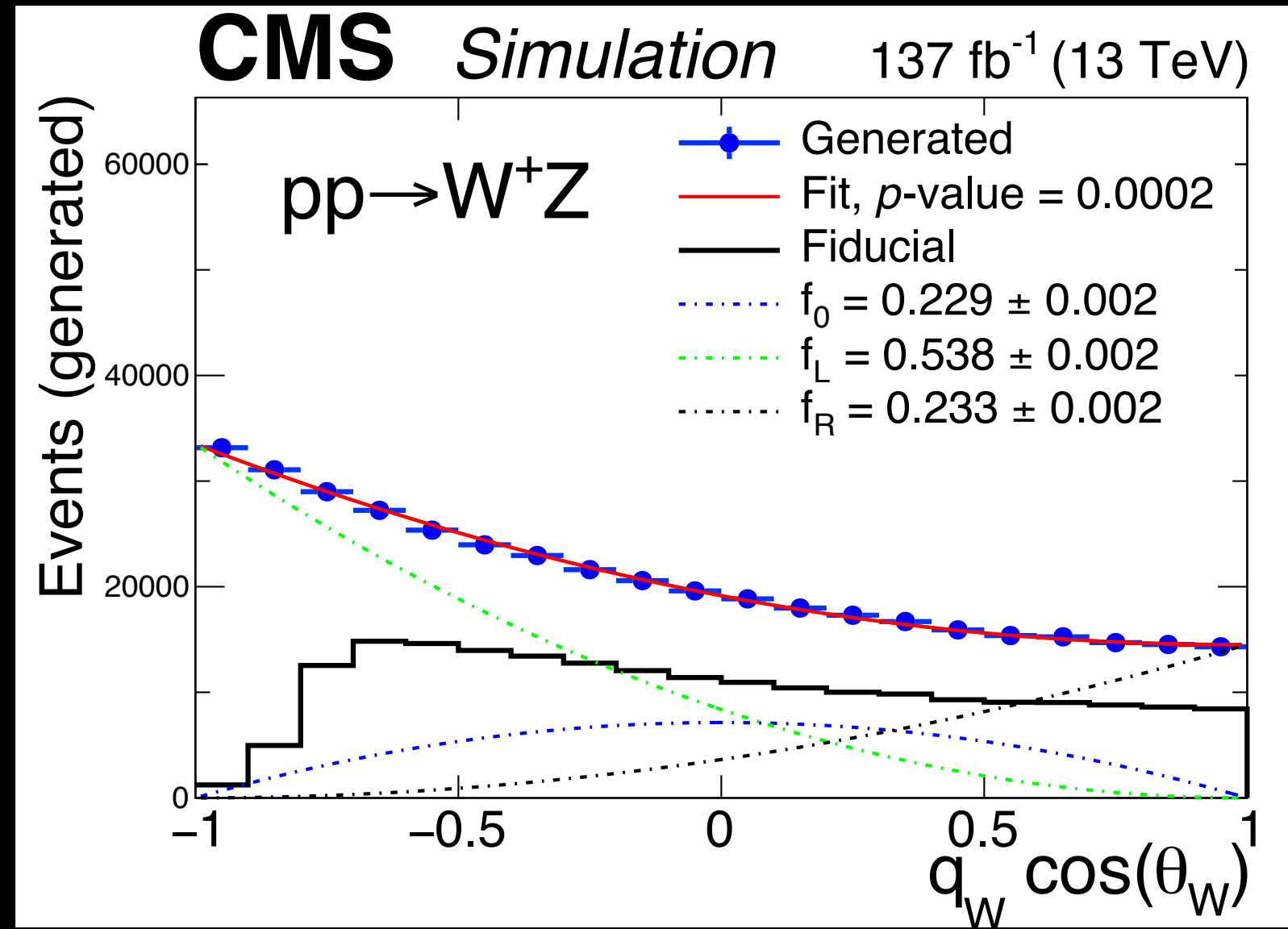
- Electroweak process: sensitive to the PDFs of u and d quarks; relatively unaffected by the gluon
- High WZ cross section makes it the dominant process that can be studied in the trilepton final state



- Ratio of $\frac{W^+Z}{W^-Z}$ cross section is one of the most precisely measurable quantities
- Constitutes first measurement of longitudinally polarized W-bosons

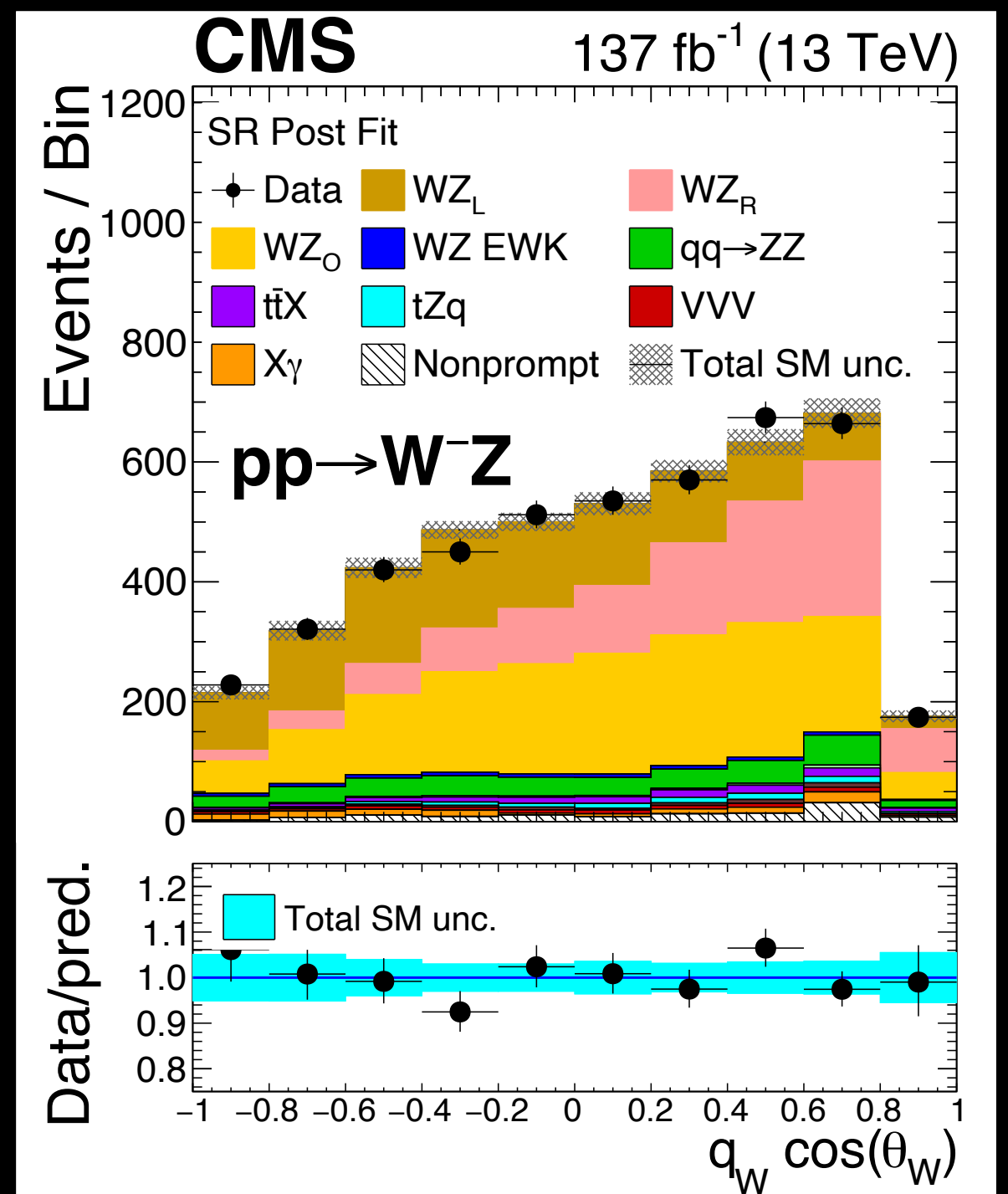
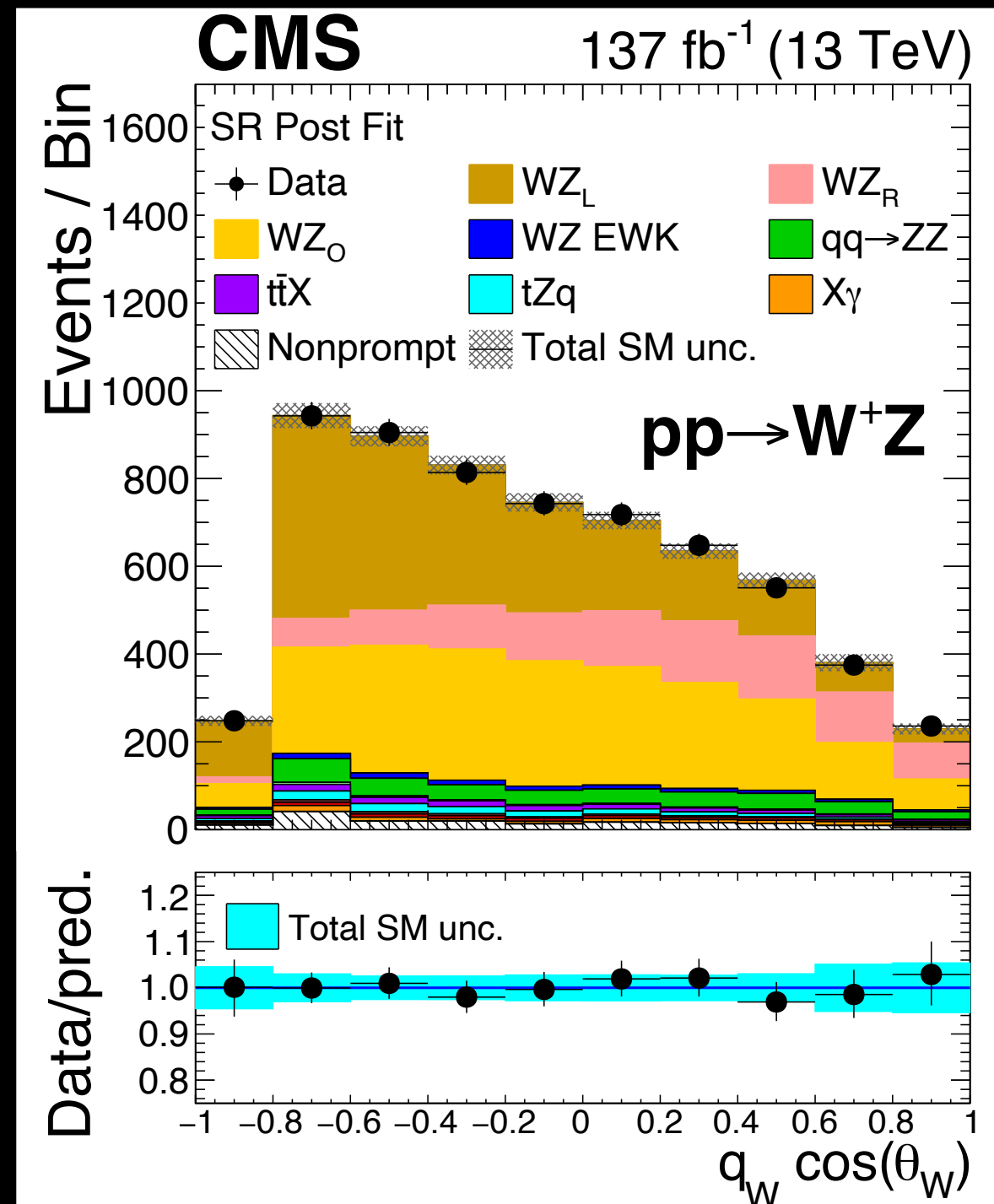
[JHEP 07 \(2022\) 032](#)

Measuring the W polarization in WZ processes

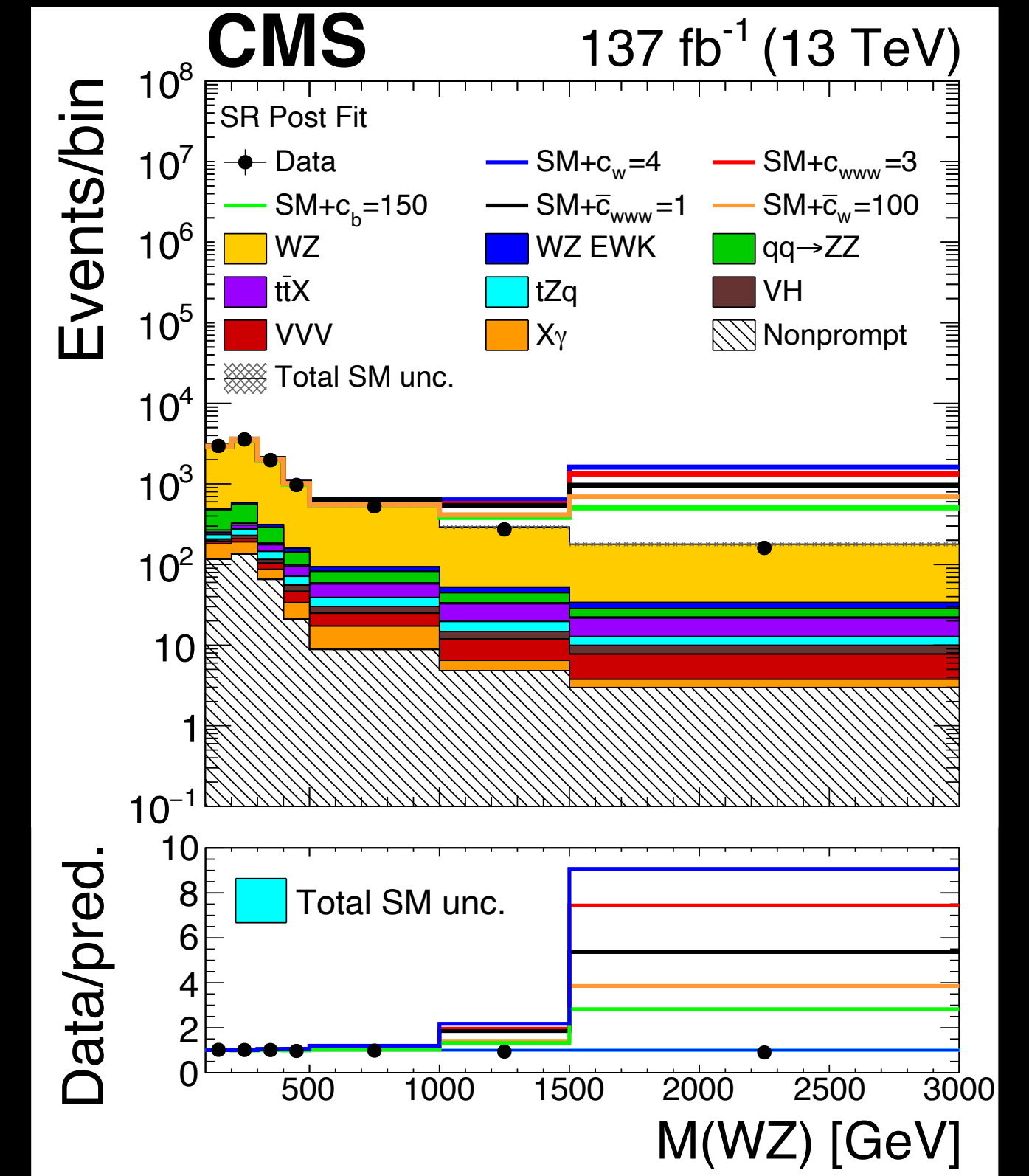
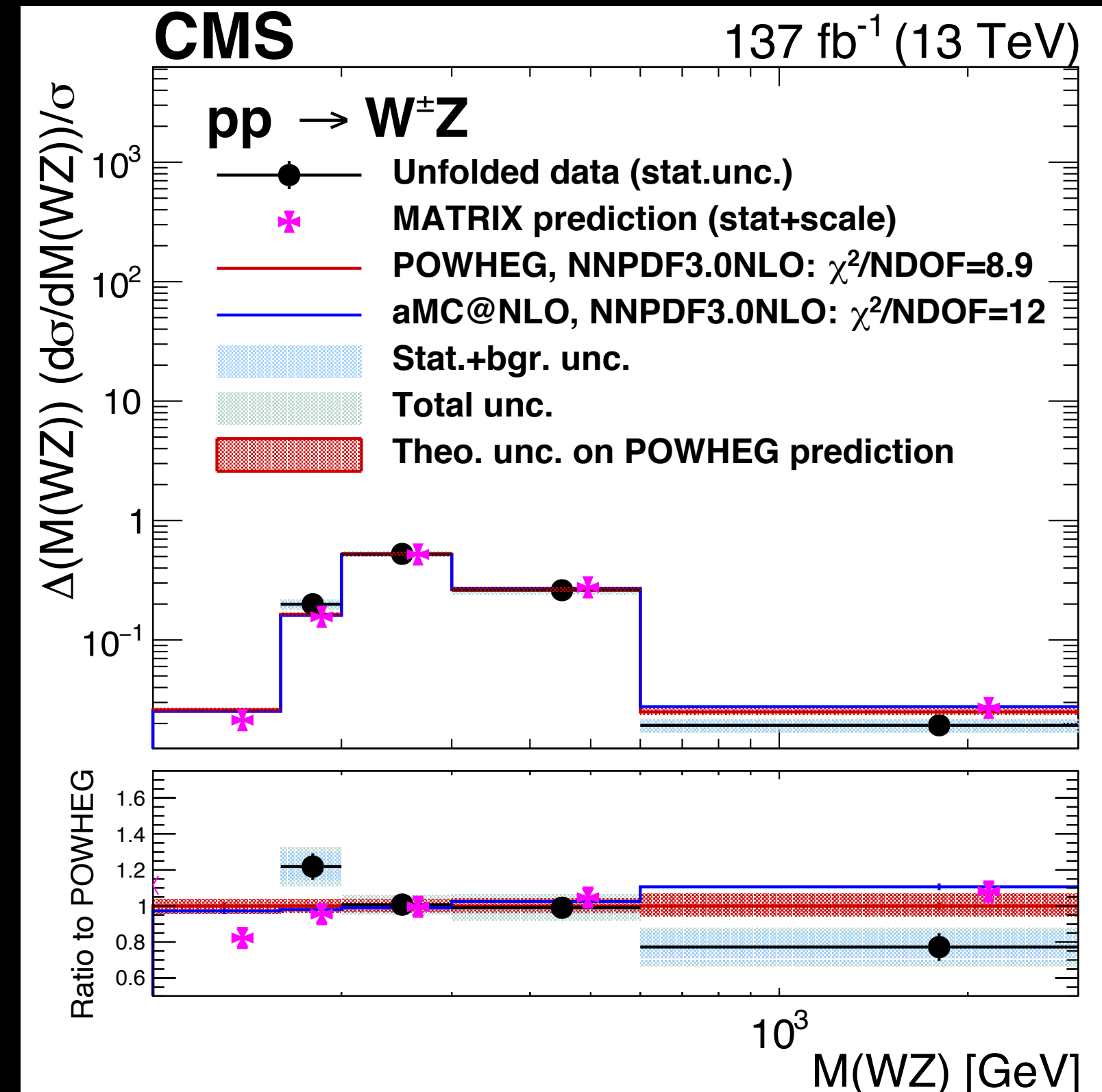
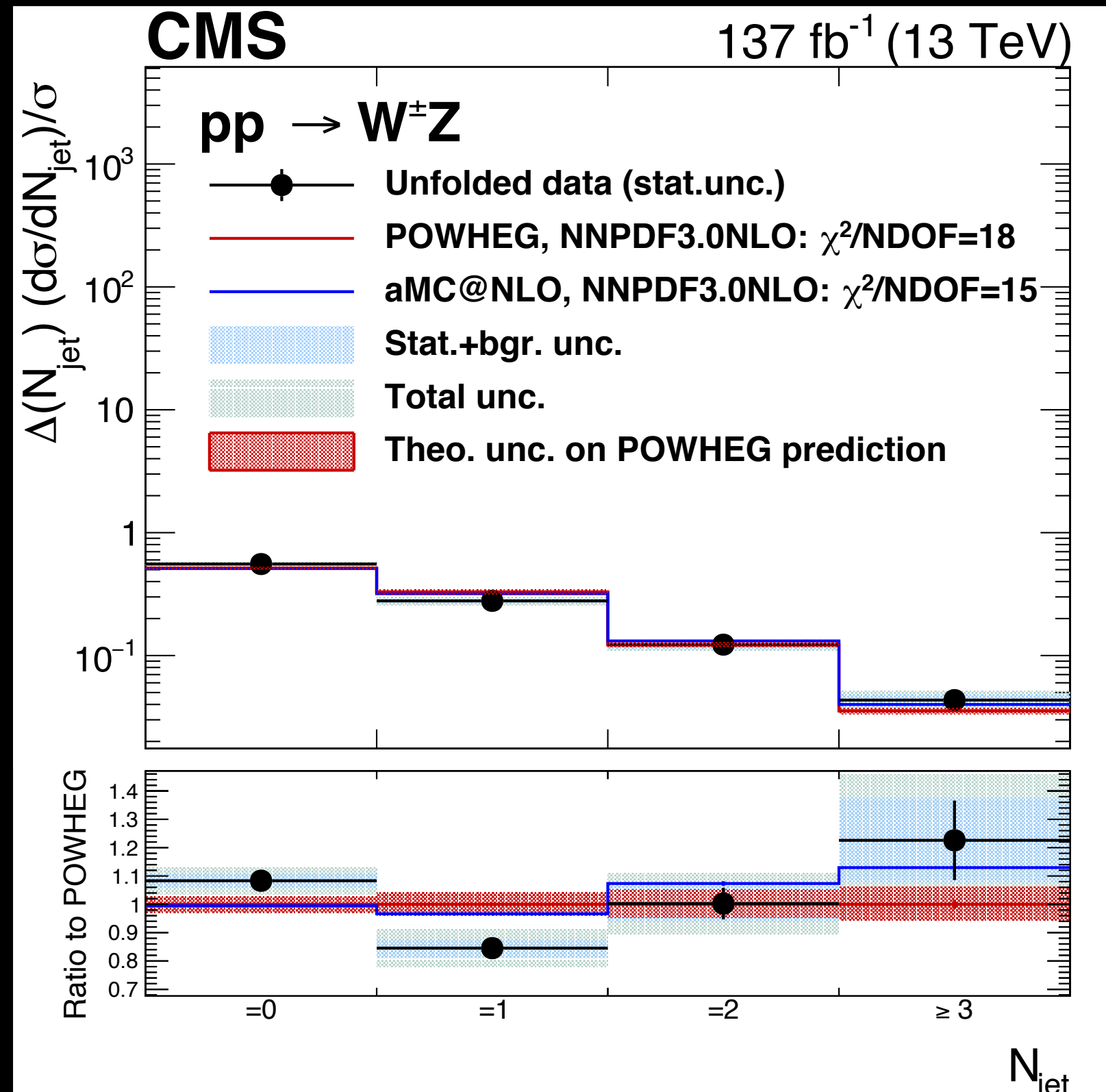


θ^W : angular distance between the momenta of the W boson and the charged lepton from its primary decay

Z



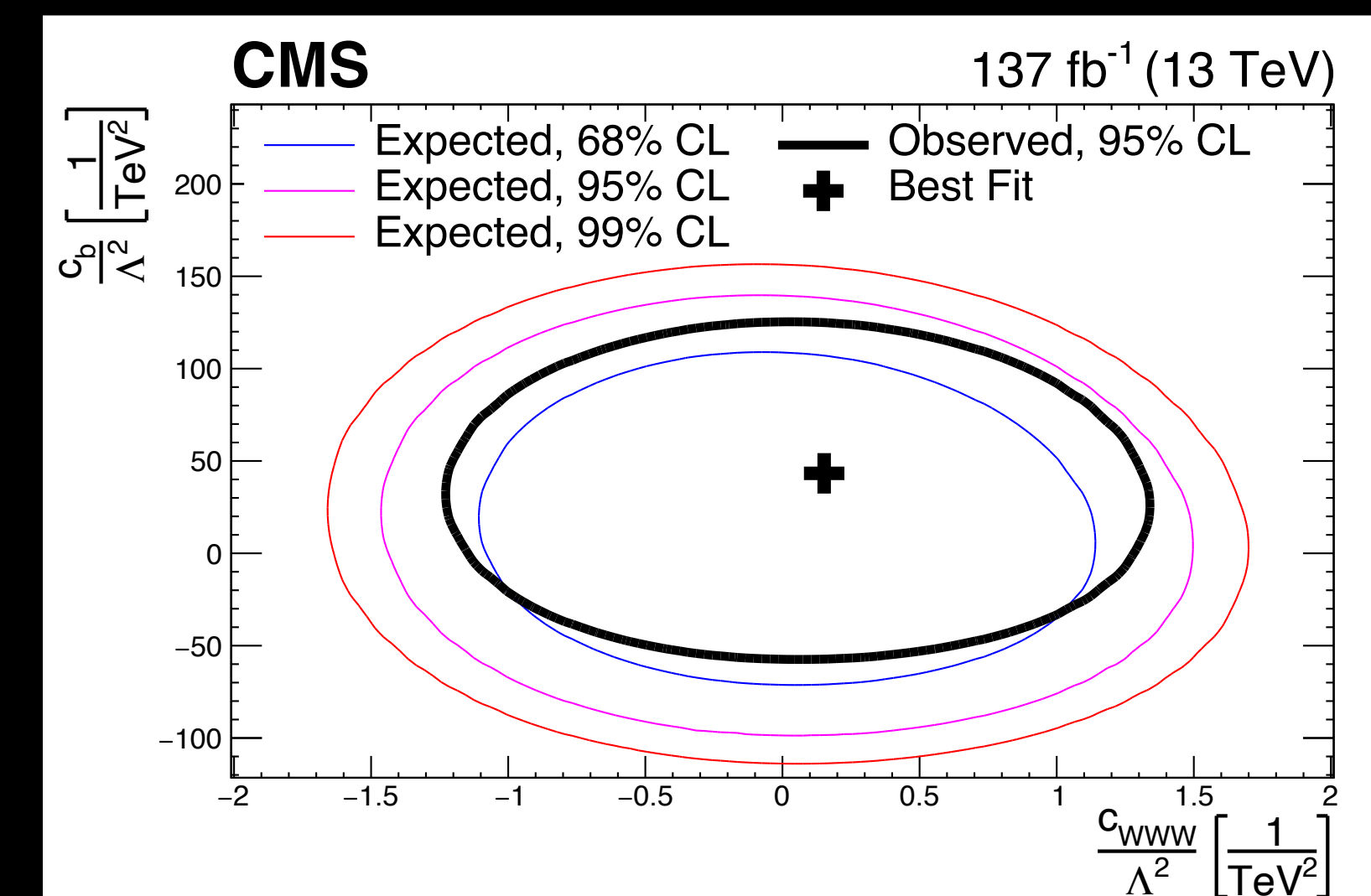
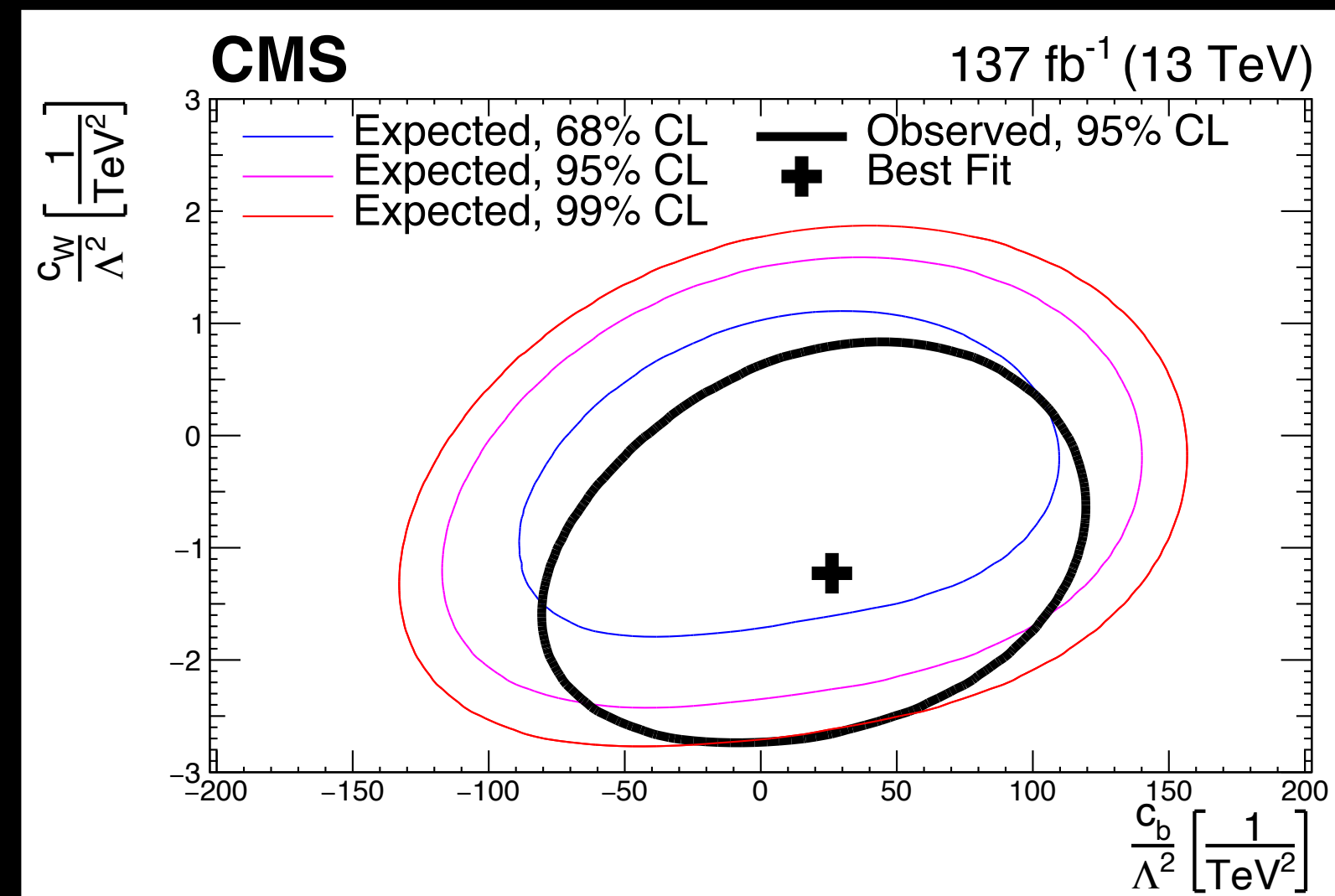
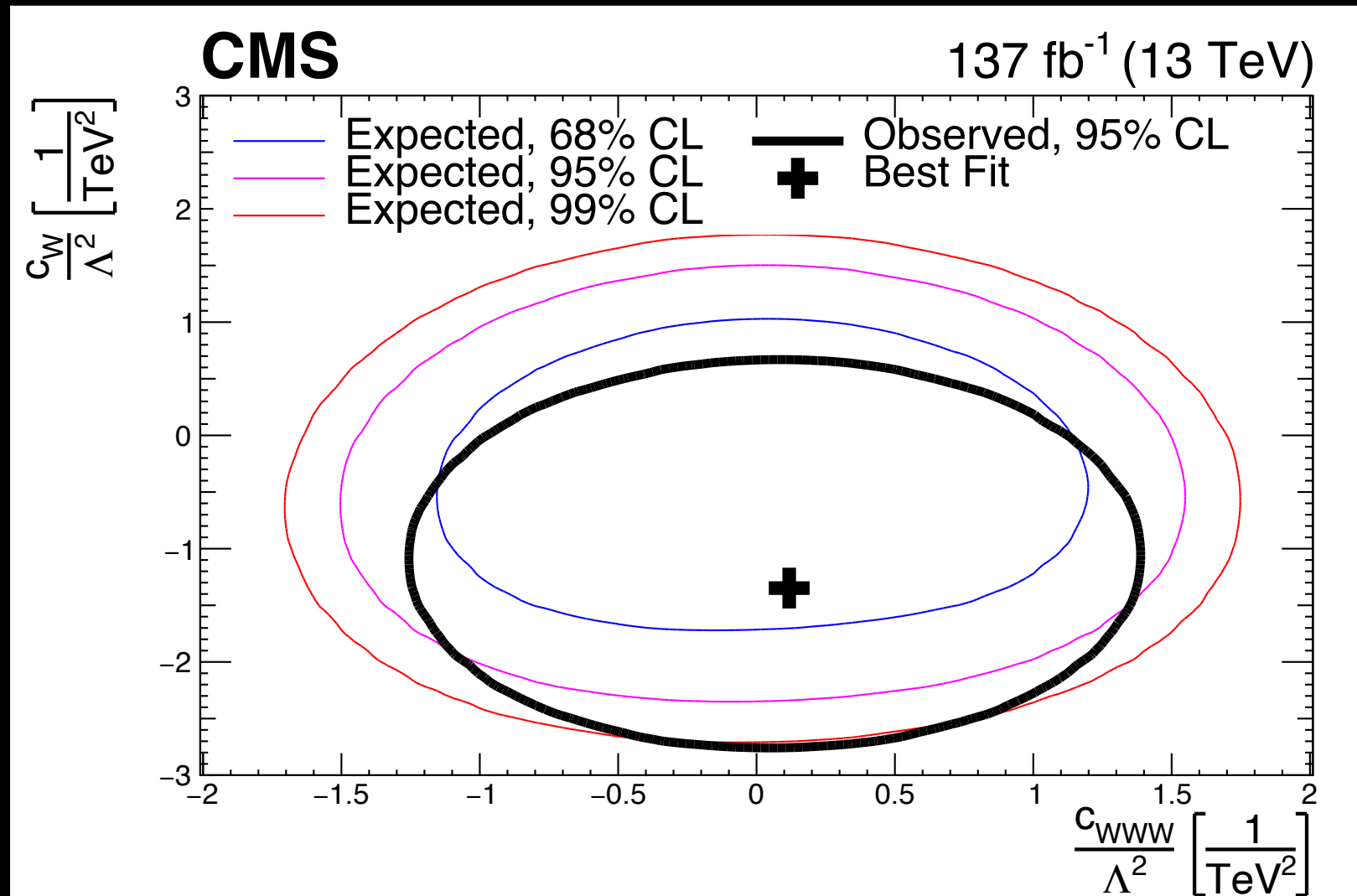
Measurement of the WZ process



- Unfolded distributions of sensitive variables well modeled
- Simulated signal samples normalized to NNLO cross sections

Effective Field Theory

$$\mathcal{L} = \mathcal{L}_{SM} + \sum_i \frac{c_i}{\Lambda^2} \mathcal{O}_i + \sum_j \frac{f_j}{\Lambda^4} \mathcal{O}_j$$



Parameter	95% CI, Exp. (TeV^{-2})	95% CI, Obs. (TeV^{-2})	Best fit, Obs. (TeV^{-2})
c_W / Λ^2	$[-2.05, 1.27]$	$[-2.52, 0.33]$	-1.34
c_{WWW} / Λ^2	$[-1.27, 1.33]$	$[-1.04, 1.19]$	0.15
c_b / Λ^2	$[-86.0, 125.0]$	$[-42.7, 113.0]$	43.6
$\tilde{c}_{WWW} / \Lambda^2$	$[-0.76, 0.65]$	$[-0.62, 0.53]$	-0.03
\tilde{c}_W / Λ^2	$[-46.1, 46.1]$	$[-45.9, 45.9]$	0.0

CP conserving
 CP non-conserving

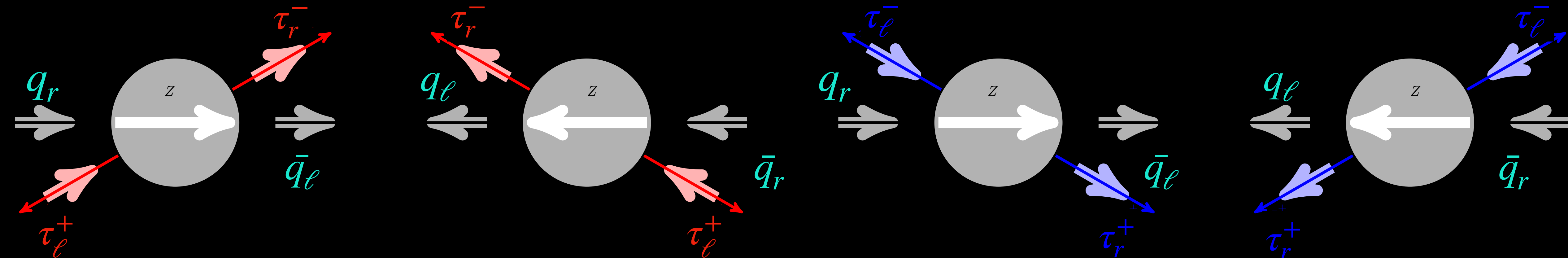
- Limits computed taking interference with SM (Λ^{-2}) + pure BSM (Λ^{-4}) into account
- Improvement over limits from W^+W^- analysis (taking luminosity scaling into account) for C_W and C_{WWW}

τ polarization in Z-boson decays

- Polarization of τ leptons is measured in $Z \rightarrow \tau\tau$ events
- Differential cross section of the $q\bar{q} \rightarrow Z \rightarrow \tau^+\tau^-$ in lowest order is expressed as:

$$\frac{d\sigma}{d\cos\theta_\tau} = F_0(\hat{s})(1 + \cos^2\theta_\tau) + 2F_1(\hat{s})\cos\theta_\tau - h_\tau[F_2(\hat{s})(1 + \cos^2\theta_\tau) + 2F_3(\hat{s})\cos\theta_\tau]$$

- Forward-backward asymmetry defined in terms of F_1 and F_2
- Polarization defined in terms of F_2 and F_0
 - Simplified when $\sqrt{\hat{s}} = M_Z$



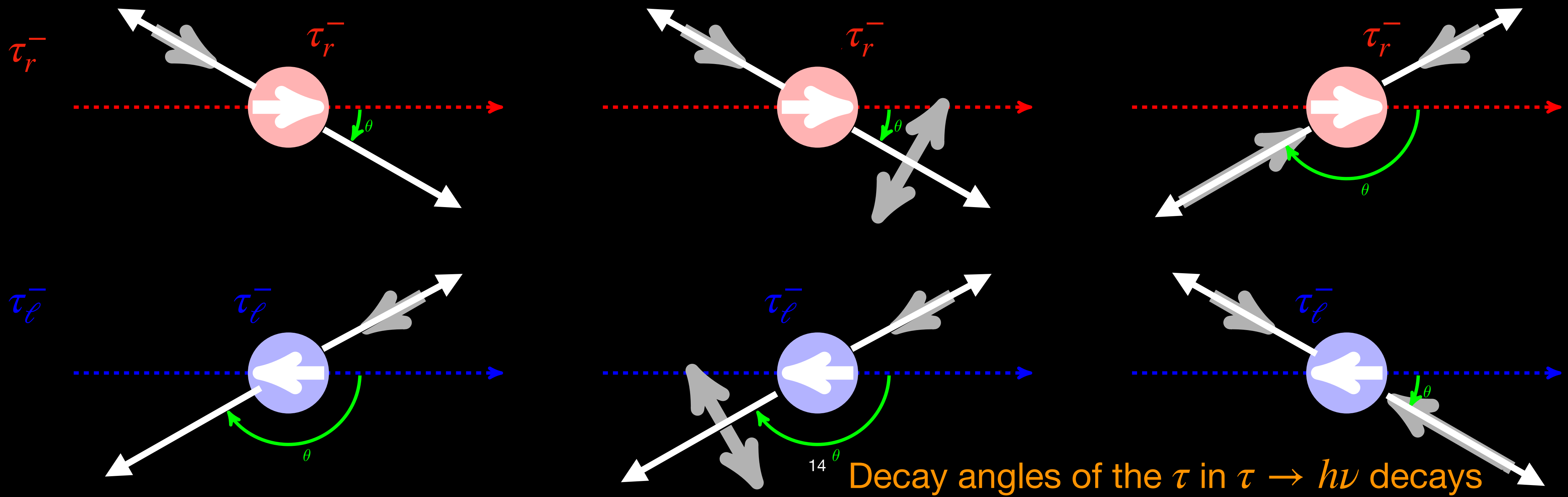
Helicity states of incoming quarks and outgoing τ leptons: thin arrows show direction of movement, thick arrows show helicity

θ_τ : scattering angle of the τ^- with respect to the quark momentum in the rest frame of the Z boson

h_τ : helicity

τ polarization in Z-boson decays

- Tau spin observables constructed from several decay angles
- Optimal observable to measure τ helicity \rightarrow polarimetric vector
 - Final-state dependent variable
 - Largest source of uncertainty from QCD normalization
- Measured value of τ polarization: $P_\tau(Z) = -0.144 \pm 0.006$ (stat) ± 0.014 (syst)
 - In agreement with LEP, SLD, ATLAS
- More precise than the previous ATLAS measurement, almost matches precision of single LEP experiments
- Weak mixing angle $\sin^2 \theta_W^{\text{eff}} = 0.2319 \pm 0.0019$ (0.8% precision)



Outlook

- Several diboson (ZZ , WZ and photon initiated processes) analyses with novel methods presented
- Comprehensive exploration of final states with a τ lepton production through the decay of Z bosons
- Diboson physics is being performed at the precision realm
- Enabling stringent tests of the electroweak gauge sector of the Standard Model

Additional Material

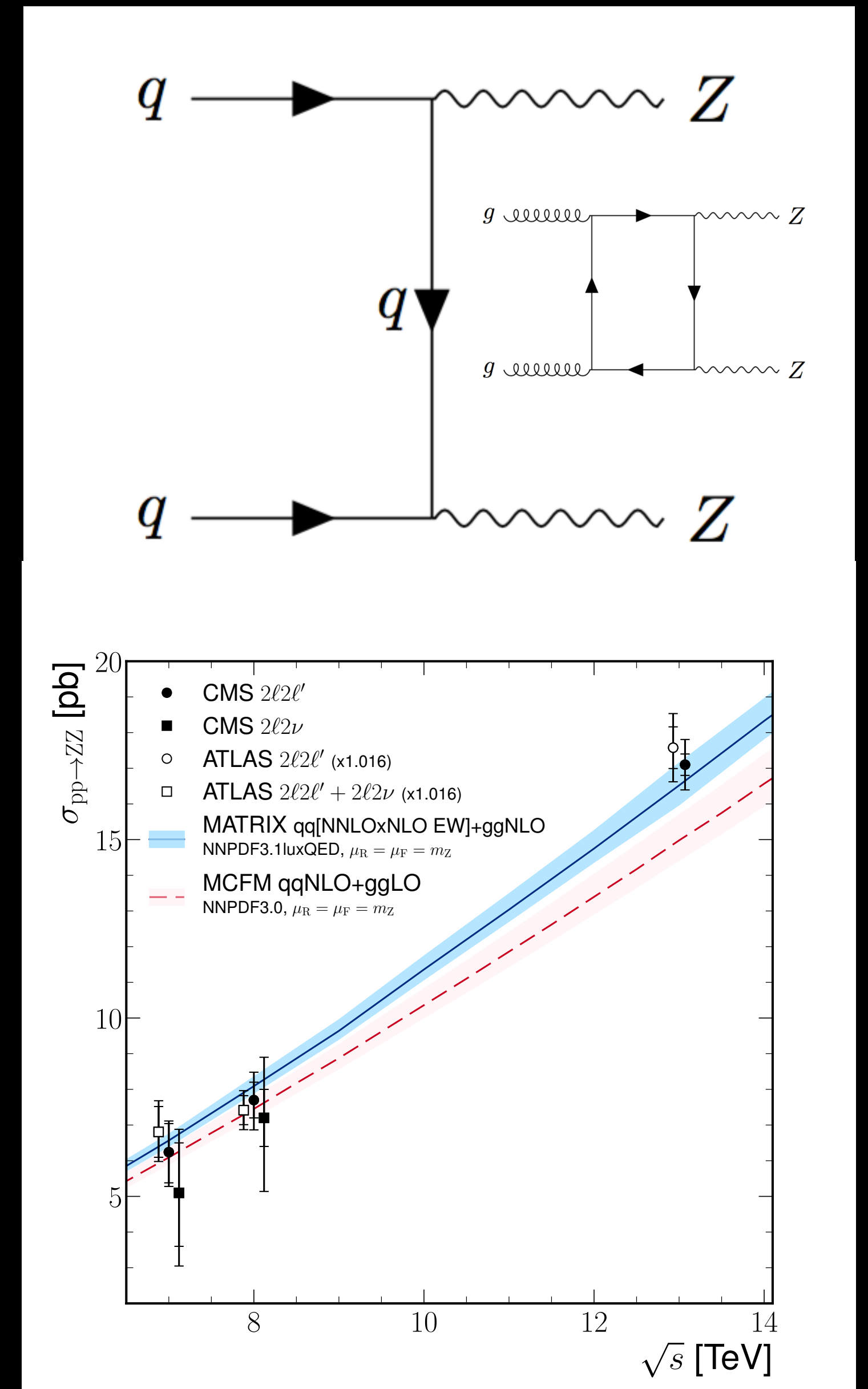
Measurement of the ZZ process

- Monte Carlo samples
 - Samples generated at NLO with Madgraph5_aMC@NLO and POWHEG
 - $gg \rightarrow ZZ$ simulated at LO with MCFM
 - Cross sections of these samples \rightarrow normalized to the cross section at NNLO for $q\bar{q} \rightarrow ZZ$ (k-factor of 1.1)
 - Cross section NLO in QCD for $gg \rightarrow ZZ$ (k-factor of 1.7)
 - nNNLO+PS: NNLO predictions for quark initiated channel combined with parton showers using the MiNNLO_{PS} method
 - NLO predictions for loop induced gluon fusion channel matched to parton showers
 - Spin correlations, interferences and off-shell effects are included by calculating the full process $pp \rightarrow \ell^+ \ell^- \ell'^+ \ell'^-$
- Unfolding
 - Used D'agostini's method (RooUnfold toolkit)

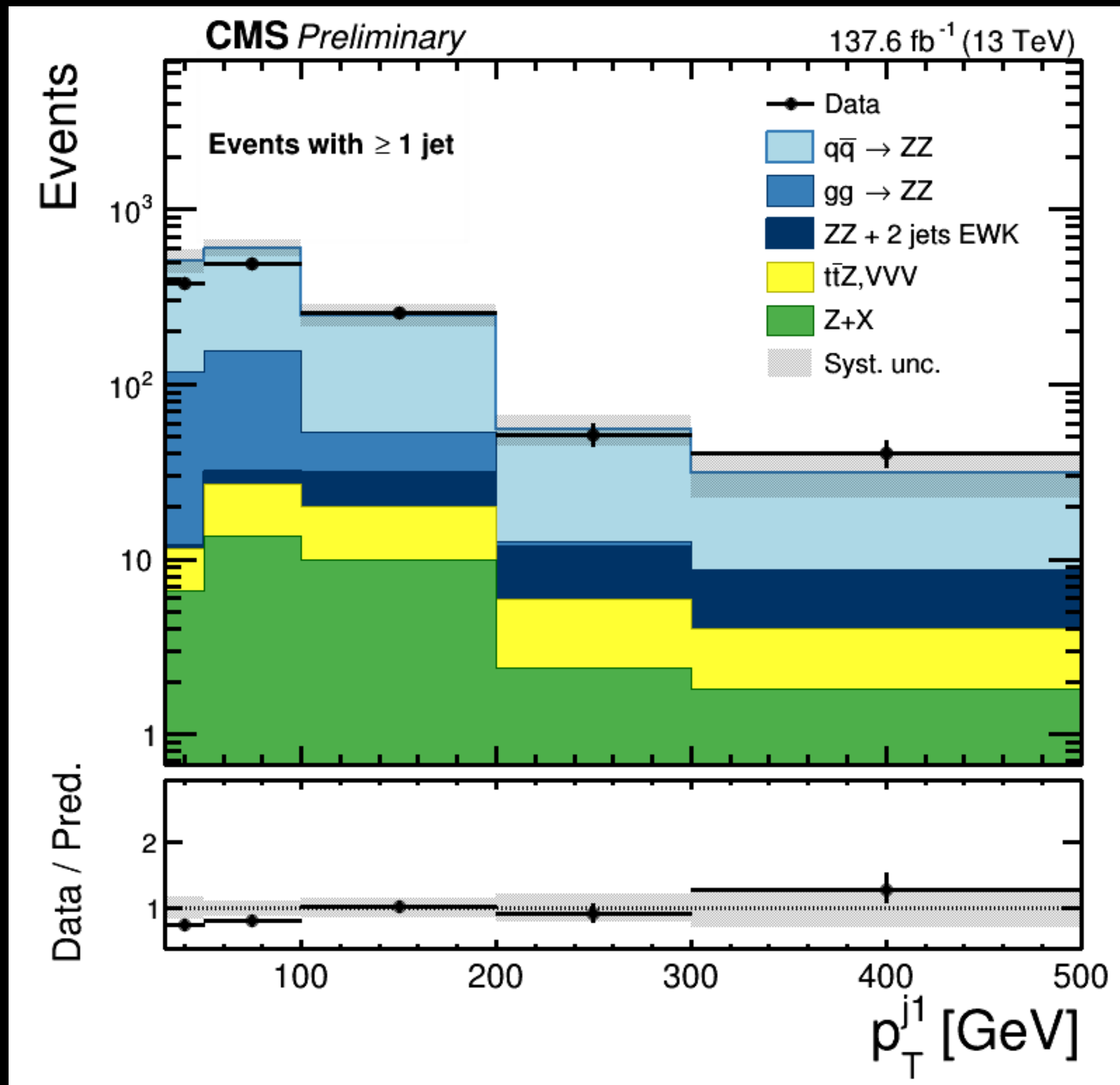
Hot off the press!

Measurement of the ZZ process

- Measurement of ZZ production in 4 lepton final state
 - No s-channel production — forbidden in the SM
 - Loop effects — up to 10% contribution
- On-shell requirement on both Z-boson candidates
- Inclusive cross section studied in detail
- **First differential cross sections measured** as a function of:
 - number of jets
 - transverse momentum (p_T)
 - pseudorapidity (η)
 - invariant mass of the highest p_T and the second highest p_T jets
 - $\Delta\eta$ of the highest p_T and the second highest p_T jets
 - m_{4l} as a function of different jet multiplicities



Measurement of the ZZ process





Search for exclusive $\gamma\gamma \rightarrow WW$ and $\gamma\gamma \rightarrow ZZ$ production in final states with jets and forward protons

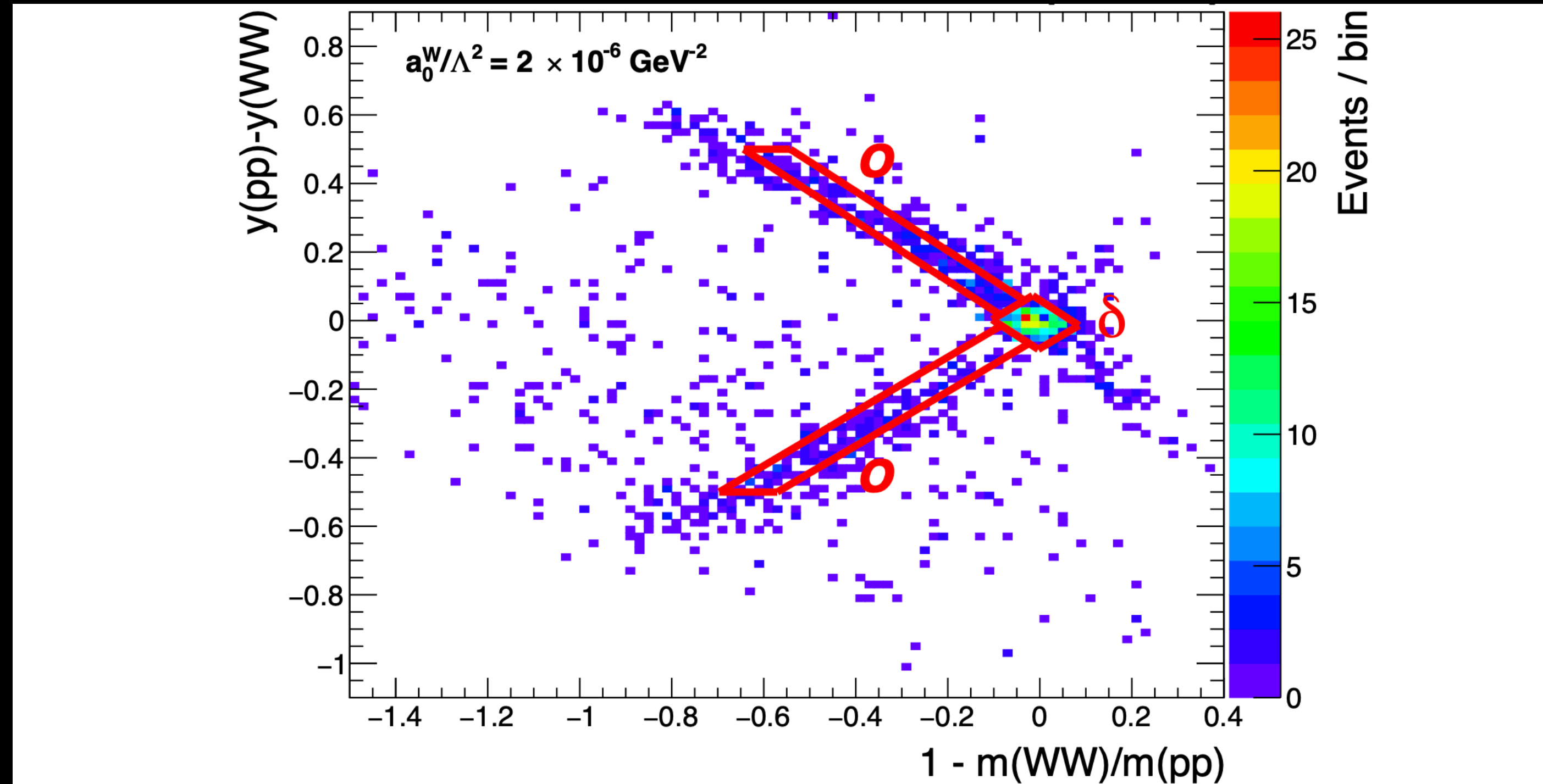
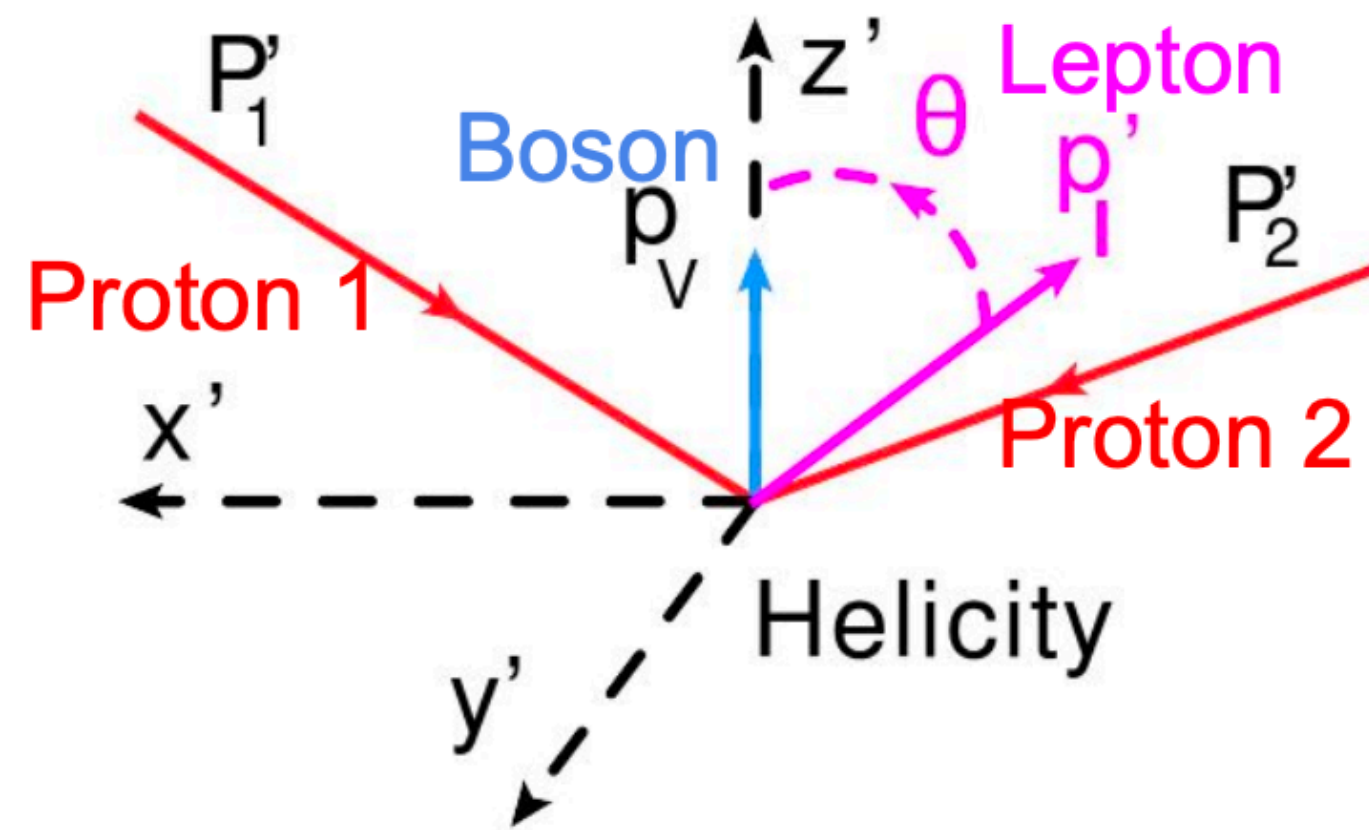
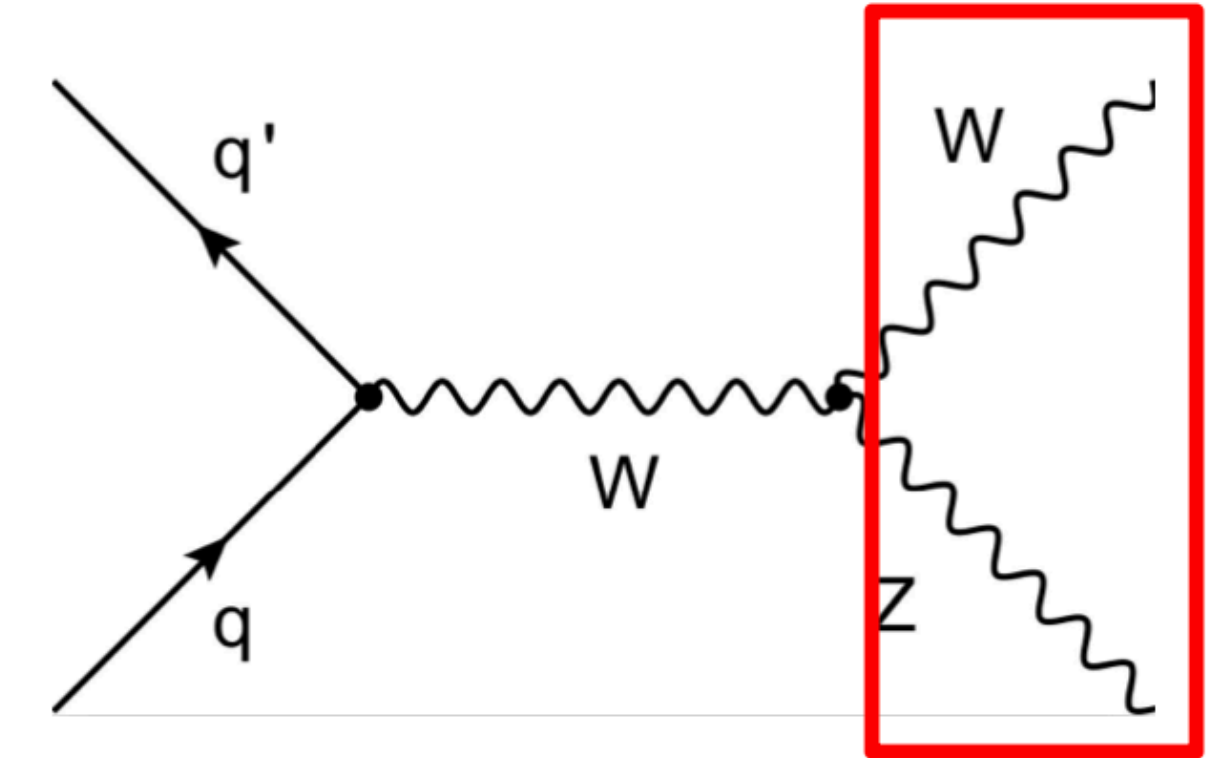


Figure 4: Matching between the jets and the protons, in invariant mass and rapidity, for simulated WW exclusive signal events. The red diamond-shaped area near the origin (signal region δ) corresponds to the case where both protons are correctly matched to the jets. The areas within the red diagonal bands (signal region o) correspond to the case where one proton is correctly matched, and the second proton originates from a pileup interaction.

Boson polarization studies - Description

→ We also look at the “final” WZ state. We study the polarization of the W and Z bosons, a measurement sensitive to possible gauge/higgs couplings anomalies.

→ The polarization is studied in terms of the polarization angle θ :



Helicity frame: the lab frame is rotated so the V boson is in the Z axis, then it is boosted such that the V boson is at rest.

→ At LO in EW the following quadratic relations hold for θ :

$$\frac{d\sigma}{\sigma d \cos \theta^Z} = \frac{3}{8} \left[(1 + \cos^2(\theta^Z) + 2c \cos(\theta^Z)) f_L^Z + (1 + \cos^2(\theta^Z) - 2c \cos(\theta^Z)) f_R^Z + 2 \sin^2(\theta^Z) f_0^Z \right]$$

→ Where f_L, f_R, f_0 are the “polarization fractions”, quantities that are related to the boson spin density matrix, and are well defined but frame-dependant as they relate to particle helicities. By construction they fulfill: $f_L + f_R + f_0 = 1$. A separate set appears for W and Z production.

→ We aim to measure the W/Z polarization fractions into the helicity frame (technically also prepared for Collins-Sopper).

τ polarization in Z-boson decays

Considering the decay $\tau^- \rightarrow \pi^- \nu$, there is no angular momentum in the two-body τ decay and since the pion carries no spin, angular momentum conservation requires the neutrino to adopt the spin of the τ lepton. In the τ lepton rest frame, the neutrino and pion are emitted back-to-back. Since the neutrino is always left-handed the π^- prefers small values for the angle θ in the decay of a right-handed τ_R and large values in case the τ lepton is left-handed. In this case the angle θ carries all spin information.

The decay into a spin-one resonance, ρ or a_1 , offers the kinematic simplicity of a two-body decay, like the $\tau^- \rightarrow \pi^- \nu$ decay, but with more complicated dynamics since the ρ and a_1 resonances can have longitudinal and transverse helicity states. Conservation of angular momentum allows for the ρ and a_1 resonances helicities to be equal to $\lambda_V = 0$ or -1 .

If the τ lepton is in the right-handed state, the V ($V = \rho, a_1$) resonance tends to be in a longitudinally polarized state ($\lambda_V = 0$). Conversely, if the τ is left-handed, the V is preferably transversely polarized, $\lambda_V = -1$. Combining the spin amplitudes for all possible configurations of the V resonance and τ helicities, one gets [35]:

$$\frac{1}{\Gamma} \frac{d\Gamma}{d \cos \theta} \propto 1 + \alpha_V h_\tau \cos \theta, \quad (8)$$

where the dilution factor $\alpha_V = (|M_L|^2 - |M_T|^2) / (|M_T|^2 + |M_L|^2) = (m_\tau^2 - 2m_V^2) / (m_\tau^2 + 2m_V^2)$ is a result of the presence of the transverse amplitude M_T of the V resonance in addition to the longitudinal amplitude M_L . The value of the factor α_V characterizes the sensitivity of the $\cos \theta$ observable. For comparison, in the τ lepton decay to the a_1 resonance, $\alpha_{a_1} = 0.021$, in the ρ decay, $\alpha_\rho = 0.46$ and in the pion decay, $\alpha_\pi = 1$. Consequently, the sensitivity to the τ lepton helicity in $\tau \rightarrow V\nu$ decays is strongly reduced if only the $\cos \theta$ angle is considered. The spin of V is transformed into the total angular momentum of the decay products and thus can be retrieved by analyzing the subsequent V decay.

τ polarization in Z-boson decays

There are two additional angles to be considered in the decay of $\tau^- \rightarrow \rho^- \nu$ ($\rho^- \rightarrow \pi^- \pi^0$): β denotes the angle between the direction of the charged pion in the ρ rest frame and the direction of the ρ , given by:

$$\cos \beta = \mathbf{q} \cdot \mathbf{n}_\rho = \frac{m_\rho}{\sqrt{m_\rho^2 - 4m_\pi^2}} \cdot \frac{E_{\pi^-} - E_{\pi^0}}{|p_{\pi^-} - p_{\pi^0}|}, \quad (9)$$

where \mathbf{q} is a unit vector along the direction of the charged pion in the ρ rest frame and \mathbf{n}_ρ is the direction of the movement of the ρ projected into its rest frame. The rotation plane of two

pions is aligned correspondingly to the spin of the ρ resonance. In the case of $\lambda_\rho = 0$, the angle β tends to small values, and to large values if $\lambda_\rho = -1$. The angle β in $\tau^- \rightarrow \rho^- \nu$ is sketched in Fig. 3b. This angle contains only quantities that can be measured directly and is a very powerful variable to discriminate left- and right-handed helicity states.

The similar, but not identical, angle β can be defined for the $\tau^- \rightarrow a_1^- \nu$. In this case β is defined as the angle between the normal to the 3π decay plane and the a_1 flight direction. The angle is shown in Fig. 3d.

A further angle α is defined by the two planes spanned by vectors $(\mathbf{n}_V, \mathbf{n}_\tau)$ and $(\mathbf{n}_V, \mathbf{q})$, respectively:

$$\cos \alpha = \frac{(\mathbf{n}_V \times \mathbf{n}_\tau) \cdot (\mathbf{n}_V \times \mathbf{q})}{|\mathbf{n}_V \times \mathbf{n}_\tau| \cdot |\mathbf{n}_V \times \mathbf{q}|}. \quad (10)$$

Here all vectors are defined in the resonance rest frame. The vector \mathbf{n}_V denotes the direction of ρ or a_1 resonance and \mathbf{n}_τ is the direction of the τ lepton. The angle α describes the correlation between the helicity of the τ lepton and the decay products of the ρ or a_1 resonance. The vector \mathbf{q} denotes the direction of the π^- in case of $\tau^- \rightarrow \rho^- \nu$ decay and π^+ in $\tau^- \rightarrow a_1^- \nu$ decay. The angle α is illustrated in Fig. 3a.

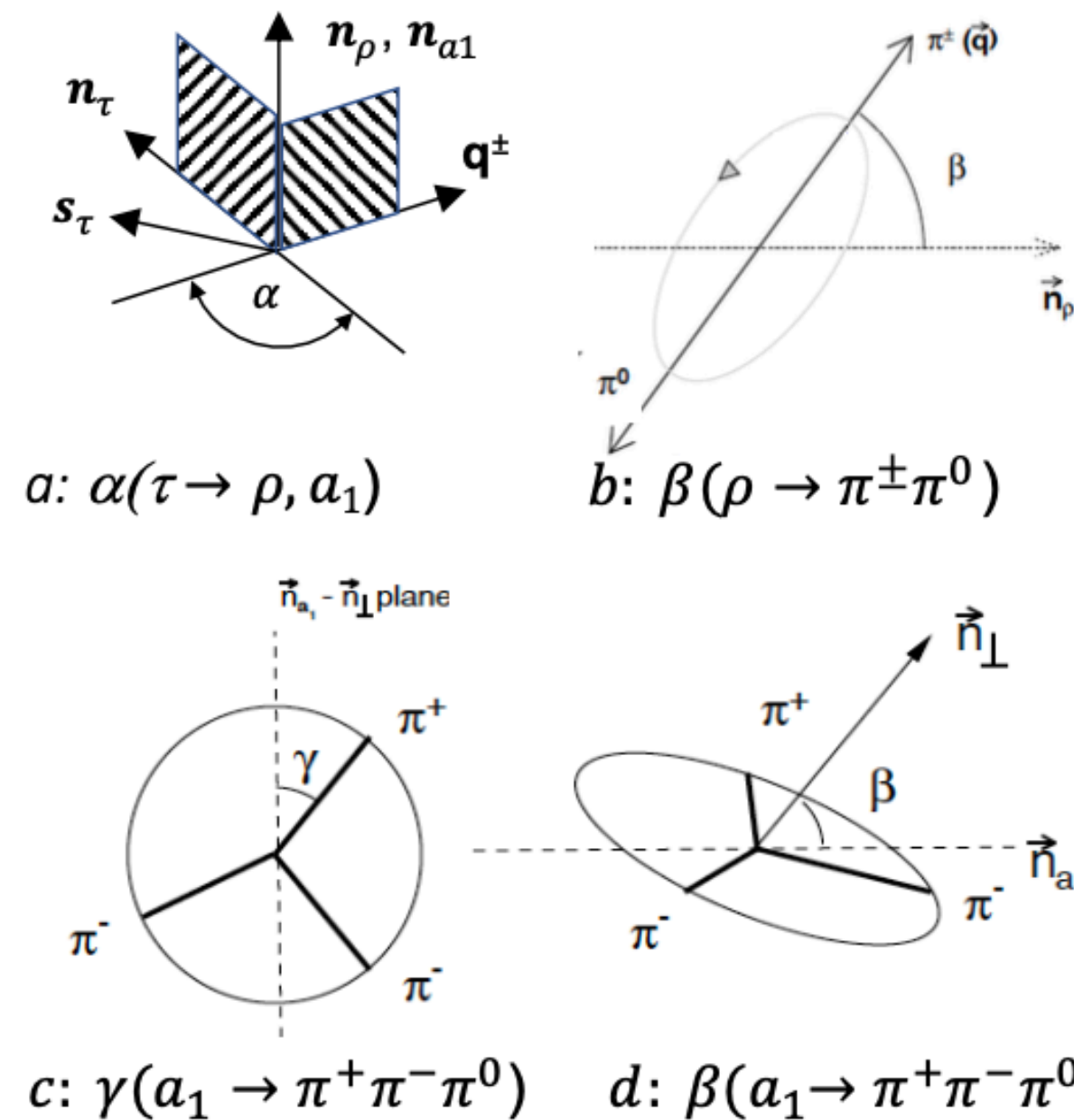


Figure 3: Definitions of the angles α in both $\tau^- \rightarrow \rho^- \nu$ and $\tau^- \rightarrow a_1^- \nu$ (a), the angle β in $\tau^- \rightarrow \rho^- \nu$ (b) and for the decay $\tau^- \rightarrow a_1^- \nu$ (d) and finally the angle (γ (c)) for the decay of $a_1^- \rightarrow \pi^- \pi^+ \pi^-$

7.2 Optimal observable

Optimal variables to measure the helicity of τ leptons have been widely explored at LEP and are explained, for example, in Ref. [36]. The idea is to replace multi-dimensional fits over all relevant decay angles by a one dimensional fit to a unique variable $\omega(\theta, \alpha, \beta, \gamma, \dots)$, which can be calculated using the squared matrix elements of the decay for positive and negative helicity. This procedure is equivalent to the use of the concept of the polarimetric vector.

In general the differential widths of any decay of a polarized τ lepton can be described using the polarimetric vector and has then the simplified form [14, 35]:

$$d\Gamma = \frac{|\overline{M}|^2}{2m_\tau} (1 - h_\mu s^\mu) d\text{LIPS}, \quad (11)$$

where $d\text{LIPS}$ is the element of Lorentz-invariant phase space, s is the four-vector of the spin of the τ lepton and h is the polarimetric vector. In the rest frame of the τ lepton, assuming that the τ lepton spin is aligned to the τ lepton flight direction (all transverse τ spin components are zero), this reads:

Table 2: Final choice of discriminators in the different event categories

Channel	Category	Discriminator	
$\tau_e \tau_\mu$	$e + \mu$	$m_{\text{vis}}(e, \mu)$	visible mass
$\tau_e \tau_h$	$e + a_1$	$\omega(a_1)$	optimal observable with SVfit
	$e + \rho$	$\omega_{\text{vis}}(\rho)$	visible optimal observable
	$e + \pi$	$\omega(\pi)$	optimal observable with SVfit
$\tau_\mu \tau_h$	$\mu + a_1$	$\omega(a_1)$	optimal observable with SVfit
	$\mu + \rho$	$\omega_{\text{vis}}(\rho)$	visible optimal observable
	$\mu + \pi$	$\omega(\pi)$	optimal observable with SVfit
$\tau_h \tau_h$	$a_1 + a_1$	$m_{\text{vis}}(a_1, a_1)$	visible mass
	$a_1 + \pi$	$\Omega(a_1, \pi)$	combined optimal observable with SVfit
	$\rho + \tau_h$	$\omega_{\text{vis}}(\rho)$	visible optimal observable (for leading ρ)
	$\pi + \pi$	$m_{\text{vis}}(\pi, \pi)$	visible mass

τ polarization in Z-boson decays

$$w = \frac{1}{4} \sum_{i,j=0}^4 h_i^+ h_j^- R_{ij} \quad (7.1)$$

where h^+ and h^- are the so-called polarimeter vectors for the τ^+ and τ^- decays, respectively, and the matrix R_{ij} describing the spin orientation of the system, in the case of a Z decay, takes the form

$$R = \begin{pmatrix} 1 & 0 & 0 & -P_\tau \\ 0 & 0 & 0 & 0 \\ 0 & 0 & 0 & 0 \\ -P_\tau & 0 & 0 & 1 \end{pmatrix} \quad (7.2)$$

Here P_τ is the tau polarization given by Equation 3.10. Equations 7.1 and 7.2 are expressed in the rest frame of the Z with the z -axis in the direction of flight of the τ^- . By inserting Equation 7.2 into Equation 7.1 one obtains

$$w = \frac{1}{4} [1 + h_z^+ h_z^- - P_\tau (h_z^+ + h_z^-)] \quad (7.3)$$